Serrano, O., … et al. (2019). Generalized continuum model for the analysis of nonlinear vibrations of taut strings with microstructure. *International Journal of Solids and Structures*, v. 164, pp.: 157-167.

DOI: https://doi.org/10.1016/j.ijsolstr.2019.01.014

Generalized continuum model for the analysis of nonlinear vibrations of taut strings with microstructure

Ó. Serrano[a,*], R. Zaera[a], J. Fernández-Sáez[a], M. Ruzzene[b,c]

[a]*Department of Continuum Mechanics and Structural Analysis, University Carlos III of Madrid, Av. de la Universidad 30, 28911 Leganés, Madrid, Spain*
[b]*School of Aerospace Engineering, Georgia Institute of Technology, Atlanta, Georgia 30332, USA*
[c]*School of Mechanical Engineering, Georgia Institute of Technology, Atlanta, Georgia 30332, USA*

Abstract

Classical continuum models are unable to capture the response of a microstructured solid when the scale effect is relevant. In vibration analysis, this limitation appears when the solid undergoes vibrations of wavelength that approaches the characteristic length of the microstructure. A discrete model may be formulated to account for this effect, but this comes at the expenses of high computational costs. For example, scale effects are relevant in strings employed in sensing applications which often rely on information gathered in the nonlinear dynamic regime. In this work, we study the dynamic behavior of a taut string modeled as a lattice of particles linked to first neighbors by linear springs. We develop an inertia-gradient generalized continuum model of the chain, which undergoes nonlinear vibrations. Unlike the corresponding classical continuum model, enrichment of the kinetic energy density with the characteristic length of the microstructure permits the model to capture short-wavelength vibrations. Comparison of the response predicted by the continuum models highlights that the generalized model provides better estimations of the dynamic response of the considered microstructured string in the nonlinear regime and at short wavelengths.

Keywords: Scale effect, Gradient continuum model, Taut string, Nonlinear Vibration, Microstructure

*Corresponding author. E-mail address: oscar.serrano@uc3m.es

1. Introduction

Classical continuum models of solids permit a faithful representation of their mechanical behavior. This statement is true when the characteristic dimensions of the underlying microstructure is significantly smaller than the scale of observation. This is the case of common problems in engineering such as in the civil or mechanical industries. In contrast, there are other engineering fields where the scale of observation is of the order of the microstructure. This is the case of nano-(micro-)electronics [1, 2], nano-biotechnology [3, 4, 5], nano-thermodynamics [6, 7], or in problems involving granular and particulate media [8].

In recent years, the interest in the nonlinear regime of these nano-/micro-scale structures has been spanned by sensing applications, where the nonlinear behavior of nano-structures has the potential to enhance the information that can be obtained from the sensor. For example, Jeong et al. [9] have shown that when geometric nonlinearity is considered, nano- or micro-mechanical resonators can overcome the narrow bandwidth limitation of linear dynamic systems. Bouchaala [10] used a nonlinear formulation of a nano-electromechanical resonator for mass sensing while Atalaya et al. [11] have shown how nano-size graphene membranes can be used in the nonlinear regime for the determination of the mass and position of an added particle. While the above studies consider beam-type and membrane-type components, studies on nano-strings include the work of Verbridge et al. [12] who presented how the resonant frequency of nano-strings allow to measuring mass with sensitivity approaching a zeptogram. Leiman et al. [13] developed a device based on a nano-string for the detection of terahertz electromagnetic radiation. Other studies related to the use of nano-strings have been developed by Qin et al. [14] and Kudaibergenov et al. [15]. In these examples, as the nano-string deflects transversely, its length, and therefore its tension, increases. Hence, nonlinear terms are required to account for stretching in the equations of motion (Nayfeh et al. [16, 17]). In these cases, classical continuum models might offer an acceptable approximation of the response of the string for long-wavelength vibrations [18]. However, once the wavelength becomes comparable to the characteristic dimensions of the underlying microstructure, classical continuum models are not appropriate to take scale effects into consideration. In nano-structures such as nano-strings, considered here as a structure where the scale effect appears due to discreteness, the formulation of appropriate models is needed. Zhang et al. [19] account

for size effects by considering the string as a 1D lattice. However, this formulation has a high computational cost. In this respect, generalized continuum models turns out to be attractive [19].

In this paper we start from a lattice model of a taut string and propose an inertia-gradient generalized continuum model with the aim of obtaining an accurate response for nonlinear vibrations at wavelengths comparable to the microstructural length. For the development of this continuum model, the methodology previously employed by Vila et al. to study the nonlinear vibrations of 1D structured solids, namely rods [20] and beams [21], is now applied to a different structural typology such as the taut string. The model will be called *axiomatic* and it will be derived from postulated forms of both kinetic and potential energies. In contrast to the classical continuum model, the enriched one takes scale effects into consideration and permits to recover the response of the classical one when the scale effects are neglected. A comparison of the equations of the generalized model with those derived through a non-standard continualization of the discrete equations of the lattice model permits to establish a relation between the corresponding parameters. Moreover, the axiomatic continuum model considers axial and transverse displacements leading to geometric nonlinearities. Also, analytical solutions are given for the response of the nonlinear string. A comparison between the responses of the different continuum models with the reference discrete one is presented to validate the proposed approach. Finally, results for short wavelengths are presented to illustrate the range of validity of the proposed model.

The paper is organized as follows. Section 1 provides a brief introduction and Section 2 formulates the discrete problem. Section 3 describes the formulation of a non-standard continualization to the discrete problem. Section 4 develops the axiomatic continuum model and Section 5 compares the dispersion curves of the linearized models. Section 6 describes the methodologies used for deriving the solution of the different models considered in this work, both discrete and continuum. Section 7 illustrates the comparison between the discrete, classical continuum and axiomatic continuum models. Finally, Section 8 summarizes the results of the work.

2. Formulation of the discrete problem

In this section we extend the lattice model of the linear taut string with microstructure developed by Zhang et al. [19] to the nonlinear behavior and

considering both axial and transverse vibration. The discrete system consists of a pinned-pinned chain of $N+2$ identical particles of mass M equally spaced at distance d, considered as the characteristic length of the underlying microstructure. Hence, the total length of the chain is $L = (N+1)d$. The reference position of n-th particle is $X_n = (n-1)d$ and $Z_n = 0$, with $n = 1, 2, ..., N+2$, in X and Z directions, respectively. Particles are linked to first neighbors by linear springs of stiffness K and are allowed to move in both axial and transverse directions (see Fig. 1). The taut chain has tension P_0 in the reference position.

Let us denote the axial and transverse displacements for n-th particle at time t as $u_n(t)$ and $w_n(t)$, respectively. Boundary conditions are defined by $u_1 = u_{N+2} = w_1 = w_{N+2} = 0$. Also, the following initial conditions are imposed to the chain:

$$u_n(0) = U_0(X_n), \qquad \dot{u}_n(0) = 0, \qquad w_n(0) = W_0(X_n), \qquad \dot{w}_n(0) = 0, \quad (1)$$

U_0 and W_0 being functions of the discrete values X_n that satisfy fixed boundary conditions at the ends.

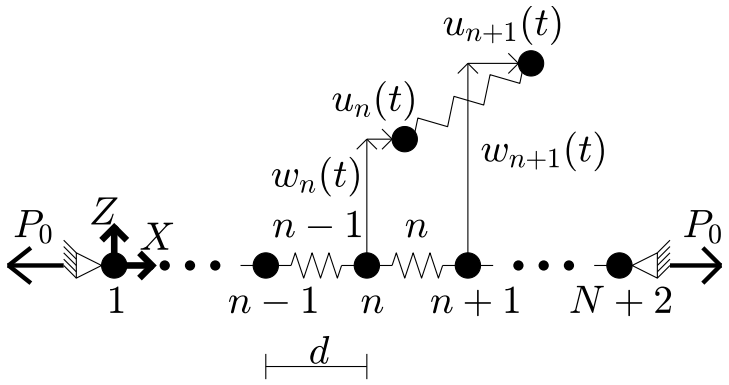

Figure 1: Sketch of the discrete model in reference and deformed position.

The kinetic energy $\mathbb{T}^{(n)}$ of the n-th particle and potential energy $\mathbb{W}^{(n)}$ of the n-th spring are defined by

$$\mathbb{T}^{(n)}_{\text{disc}} = \frac{1}{2}M\dot{u}_n^2 + \frac{1}{2}M\dot{w}_n^2, \quad (2)$$

$$\mathbb{W}^{(n)}_{\text{disc}} = \frac{1}{2}K\Delta L_n^2 + P_0\Delta L_n, \quad (3)$$

where $(\dot{\bullet})$ represents time-derivative, while ΔL_n is the elongation of the n-th spring (see Fig. 1), defined as

$$\Delta L_n = \sqrt{(u_{n+1} - u_n + d)^2 + (w_{n+1} - w_n)^2} - d. \tag{4}$$

The Lagrangian of the finite discrete model can be written as

$$\mathbb{L}_{\mathrm{D}} = \sum_n \mathbb{T}^{(n)}_{\mathrm{disc}} - \sum_n \mathbb{W}^{(n)}_{\mathrm{disc}}. \tag{5}$$

The stability of the equilibrium at the reference position can be demonstrated from the definition of the total potential energy (in absence of external loads)

$$\Pi_e = \sum_n \mathbb{W}^{(n)}_{\mathrm{disc}}, \tag{6}$$

since its first variation $\delta\Pi_e$ is zero and the second variation $\delta^2\Pi_e$ is strictly positive.

Moreover, applying Hamilton's Principle and the Fundamental Lemma of Variational Calculus leads to the following system of equations of motion for the particles

$$M\ddot{u}_n + (K\Delta L_{n-1} + P_0)\frac{d + u_n - u_{n-1}}{d + \Delta L_{n-1}} - (K\Delta L_n + P_0)\frac{d + u_{n+1} - u_n}{d + \Delta L_n} = 0, \tag{7}$$

$$M\ddot{w}_n + (K\Delta L_{n-1} + P_0)\frac{w_n - w_{n-1}}{d + \Delta L_{n-1}} - (K\Delta L_n + P_0)\frac{w_{n+1} - w_n}{d + \Delta L_n} = 0. \tag{8}$$

3. Non-standard continualization of the discrete problem

In this section we develop a non-standard continualization of the discrete system based on pseudo-differential operators [22, 23]. To this aim, we introduce the shift operator

$$\mathrm{e}^{d\partial_X} = 1 + d\partial_X + \frac{d^2}{2}\partial_X^2 + O(d^3) \tag{9}$$

which relates the displacements between neighboring particles as $u_{n+1} = \mathrm{e}^{d\partial_X} u_n$ and $w_{n+1} = \mathrm{e}^{d\partial_X} w_n$ ($\partial_X \equiv \frac{\partial}{\partial X}$). Let us define two variables $u(X,t)$, $w(X,t)$ as follows

$$\frac{\partial u}{\partial X} = \frac{u_{n+1} - u_n}{d}, \qquad \frac{\partial w}{\partial X} \equiv w' = \frac{w_{n+1} - w_n}{d}. \tag{10}$$

Variables $u(X,t)$ and $w(X,t)$ represent the continuum axial and transverse displacements at position X and time t, respectively. Then, a relation between the discrete and continuum variables can be established via Eqs. (9,10) as [23]

$$u_n = \mathbb{Q}u, \qquad w_n = \mathbb{Q}w \tag{11}$$

with

$$\mathbb{Q}(\partial_X) = \frac{d\partial_X}{\mathrm{e}^{d\partial_X} - 1} = 1 - \frac{d}{2}\partial_X + \frac{d^2}{12}\partial_X^2 + O(d^4).$$

The kinetic energy defined in Eq. (2) can now be expressed in terms of u and w by using the following relations proposed by Rosenau [23]

$$\dot{u}_n^2 = (\mathbb{Q}\dot{u}, \mathbb{Q}\dot{u}) = \int \dot{u}\mathbb{Q}^*\mathbb{Q}\dot{u}dX = \dot{u}^2 + \frac{d^2}{12}(\dot{u}')^2 + O(d^4), \tag{12}$$

$$\dot{w}_n^2 = (\mathbb{Q}\dot{w}, \mathbb{Q}\dot{w}) = \int \dot{w}\mathbb{Q}^*\mathbb{Q}\dot{w}dX = \dot{w}^2 + \frac{d^2}{12}(\dot{w}')^2 + O(d^4), \tag{13}$$

where $\mathbb{Q}^* = \mathbb{Q}(-\partial_X)$, while $(\bullet)'$ denotes derivative with respect to X. Then, by keeping terms up to order 2 in d, we obtain the approximate continuum Lagrangian

$$\mathbb{L}_{\mathrm{NS}} = \int_L \Big(\mathbb{T}_{\mathrm{cont}} - \mathbb{W}_{\mathrm{cont}}\Big)dX, \tag{14}$$

where

$$\mathbb{T}_{\mathrm{cont}} = \frac{1}{2}\frac{M}{d}\Big[\dot{u}^2 + \frac{d^2}{12}(\dot{u}')^2 + \dot{w}^2 + \frac{d^2}{12}(\dot{w}')^2\Big], \tag{15}$$

$$\mathbb{W}_{\mathrm{cont}} = \frac{1}{2}Kd(\sqrt{(u'+1)^2 + w'^2} - 1)^2 + P_0(\sqrt{(u'+1)^2 + w'^2} - 1). \tag{16}$$

Developing a Taylor-based asymptotic expansion to $\mathbb{W}_{\mathrm{cont}}$ up to fourth power terms of the derivatives, and applying Hamilton's Principle along with the Fundamental Lemma of Variational Calculus, leads to the continualized equations of motion of the discrete system

$$\ddot{u} - \frac{d^2}{12}\ddot{u}'' - \frac{Kd^2}{M}u'' - \Big(\frac{Kd^2}{M} - \frac{P_0 d}{M}\Big)\frac{\partial}{\partial X}\Big[w'^2\Big(\frac{1}{2} - u'\Big)\Big] = 0, \tag{17}$$

$$\ddot{w} - \frac{d^2}{12}\ddot{w}'' - \frac{P_0 d}{M}w'' - \Big(\frac{Kd^2}{M} - \frac{P_0 d}{M}\Big)\frac{\partial}{\partial X}\Big[w'(u' - u'^2 + \frac{1}{2}w'^2)\Big] = 0, \tag{18}$$

and the essential boundary conditions $u = 0$ and $w = 0$ at the ends.

In the next section, the governing equations of the axiomatic continuum model of a structured taut string will be compared with Eqs. (17,18) to establish a relation between the parameters of the discrete and axiomatic models.

4. Axiomatic continuum model

As stated before, classical continuum models are unable to capture the behavior of discrete problems when working with wavelengths of the order of the characteristic length of the underlying microstructure.

In this section a generalized continuum model of a taut string is presented. The model is formulated with a Mindlin-based kinetic energy [24] and a classical potential energy based on Biot strain and stress tensors [25]. The Mindlin micro-inertia term is expected to capture well wave dispersion phenomena in solids with microstructure, as stated by Mindlin [24] and Germain [26]. More recent literature related to this subject can be found in the works of Askes and Aifantis [27, 28] and Papargyri-Beskou et al. [29]. The potential energy is postulated by considering Biot strain which leads to strain expressions employed by other authors (Anand [18], Nayfeh et al. [16, 17] and Leissa et al. [30]) to obtain the governing equations of the classical nonlinear string. To this end, we first define $\mathbf{X}$ and $\mathbf{x}(\mathbf{X}, t)$ as the position vectors of a particle of the solid in the initial and current configurations, respectively. Then, the displacement vector $\mathbf{U}(\mathbf{X}, t)$ can be obtained as

$$\mathbf{U}(\mathbf{X}, t) = \mathbf{x}(\mathbf{X}, t) - \mathbf{X}. \tag{19}$$

The deformation gradient $\mathbf{F}$ can be written as follows

$$\mathbf{F} = \nabla[\mathbf{X} + \mathbf{U}(\mathbf{X}, t)] = \mathbf{I} + \nabla[\mathbf{U}(\mathbf{X}, t)], \tag{20}$$

where ∇ is the gradient operator with respect to $\mathbf{X}$, and $\mathbf{I}$ is the identity tensor.

The Biot strain tensor $\mathbf{e}$ [25] is defined as

$$\mathbf{e}(\mathbf{X}, t) = \sqrt{\mathbf{F}^{\mathrm{T}}\mathbf{F}} - \mathbf{I}. \tag{21}$$

The kinetic and potential energy densities are now postulated. The *kinetic energy density* is based on the Mindlin theory [24] which employs a scale

parameter χ, whose physical dimension is length, that accounts for the micro-inertia and the gradient of the velocities

$$\mathbb{T}_{\text{axiom}} = \frac{1}{2}\rho\Big[\frac{\partial \mathbf{U}}{\partial t}\cdot\frac{\partial \mathbf{U}}{\partial t} + \chi^2\frac{\partial(\nabla\mathbf{U})}{\partial t} : \frac{\partial(\nabla\mathbf{U})}{\partial t}\Big] \tag{22}$$

where ρ is the volumetric density. Also, "$\cdot$" and "$:$" denote the scalar product and the inner product, respectively. The typical values of χ are of the order of the characteristic dimension of the microstructure.

The *potential energy density* is based on the Biot strain tensor [25] and the potential energy introduced by the tension in the reference position through $\mathbf{T}_0$

$$\mathbb{W}_{\text{axiom}} = \frac{1}{2}\Lambda(\text{tr}\mathbf{e})^2 + \mu\mathbf{e} : \mathbf{e} + \mathbf{T}_0 : \mathbf{e} \tag{23}$$

with Lamé constants Λ and μ. Then, the Biot stress tensor including the stress component in the reference position is defined as

$$\mathbf{T}(\mathbf{X},t) = \frac{\partial \mathbb{W}}{\partial \mathbf{e}(\mathbf{X},t)} = \Lambda(\text{tr}\mathbf{e}(\mathbf{X},t))\mathbf{I} + 2\mu\mathbf{e}(\mathbf{X},t) + \mathbf{T}_0. \tag{24}$$

For the case of a unidimensional string undergoing axial and transverse displacements $\mathbf{U} = [u(X,t)\ w(X,t)]^T$, and the Biot strain is obtained by neglecting undesired deformation terms [31]

$$\text{e} = \sqrt{(1+u')^2 + w'^2} - 1. \tag{25}$$

If the string cross-section A is considered to remain undeformed (Poisson's ratio $\nu = 0$) and the stress in the reference position is $T_0 = P_0/A$, the kinetic $\mathbb{T}$ and potential $\mathbb{W}$ energy densities of the axiomatic continuum model are given by

$$\mathbb{T}_{\text{axiom}} = \frac{1}{2}\rho\Big[\dot{u}^2 + \dot{w}^2 + \chi^2(\dot{u}'^2 + \dot{w}'^2)\Big], \tag{26}$$

$$\mathbb{W}_{\text{axiom}} = \frac{1}{2}E\text{e}^2 + \frac{P_0}{A}\text{e} \tag{27}$$

with Young modulus E. As for the discrete model, it can be shown that the reference position is in stable equilibrium.

The Lagrangian of the axiomatic continuum model is obtained from

$$\mathbb{L}_{\text{AX}} = \int_L \mathbb{T}_{\text{axiom}} - \mathbb{W}_{\text{axiom}} dX. \tag{28}$$

Developing a Taylor-based asymptotic expansion to $\mathbb{W}_{\text{axiom}}$ up to fourth order and applying Hamilton's principle yields the governing equations for the axial and transverse displacements u and w

$$\ddot{u} - \chi^2 \ddot{u}'' - c_1^2 u'' - \left(c_1^2 - c_2^2\right) \frac{\partial}{\partial x}\left[w'^2\left(\frac{1}{2} - u'\right)\right] = 0, \tag{29}$$

$$\ddot{w} - \chi^2 \ddot{w}'' - c_2^2 w'' - \left(c_1^2 - c_2^2\right) \frac{\partial}{\partial x}\left[w'(u' - u'^2 + \frac{1}{2}w'^2)\right] = 0, \tag{30}$$

where $c_1^2 = \frac{E}{\rho}$, $c_2^2 = \frac{P_0}{\rho A}$, with essential boundary conditions $u = 0$ and $w = 0$ at the ends. For $\chi = 0$, the classical nonlinear continuum equations of a nonlinear taut string are recovered (Nayfeh et al. [16]). It is important to highlight that the classical nonlinear continuum equations can be obtained from a Taylor-based continualization of Eqs. (7,8). This suggests that the considered lattice model is representative of the dynamic behavior of the string.

Let us compare continualized (17, 18) and axiomatic (29, 30) equations. It is straightforward to see that these equations are identical when

$$\frac{Kd^2}{M} = \frac{E}{\rho}, \qquad \frac{M}{d} = \rho A, \qquad \frac{d^2}{12} = \chi^2. \tag{31}$$

Therefore, these relations establish the link between the discrete and continuum parameters. In particular, the scale parameter χ can be obtained from the physical characteristics of the discrete system. Anand et al. [18] and Nayfeh et al. [17] have shown the existence of interactions between axial and transverse modes of vibration. The i-th axial mode interacts with the j-th transverse one when $ic_1 \approx 2jc_2$. For the case of $c_2^2/c_1^2 << 1$ that is when the stiffness of the string EA is much higher than the tension P_0 in the reference position, and assuming lower-order transverse modes, this interaction is not present and the axial inertia $\ddot{u}$ (and $\ddot{u}''$) is therefore negligible (Nayfeh et al. [17]). Hence Eq. (29) can be approximated to

$$u'' = -\frac{\partial}{\partial X}\left[w'^2\left(\frac{1}{2} - u'\right)\right]. \tag{32}$$

Integrating Eq. (32) twice by considering $w'^2 << 1$ and $u(0,t) = u(L,t) = 0$, gives

$$u = \frac{X}{2L}\int_0^L w'^2 dX - \frac{1}{2}\int_0^X w'^2 dX. \tag{33}$$

Finally, substituting Eq. (33) into Eq. (30), neglecting c_2^2 compared to c_1^2 and keeping cubic terms of w leads to the equation for transverse motion in the following form

$$\ddot{w} - \chi^2 \ddot{w}'' - c_2^2 w'' - \frac{c_1^2}{2L} w'' \int_0^L w'^2 dX = 0. \tag{34}$$

Note that Eq. (34) takes the scale effect under consideration. For $\chi = 0$, the corresponding nonlinear classical continuum equation after applying the above-mentioned assumptions is recovered [16, 17, 18].

5. Comparison of linear models

In this section we analyze the dispersion curves of the linear versions of the discrete, classical continuum and axiomatic continuum models. Even though the linear regime is here considered, the comparison between them provides an insight useful for the nonlinear regime.

The governing equations for the linear discrete model are

$$M\ddot{u}_n - K(u_{n+1} - 2u_n + u_{n-1}) = 0, \tag{35}$$

$$M\ddot{w}_n - \frac{P_0}{d}(w_{n+1} - 2w_n + w_{n-1}) = 0, \tag{36}$$

which are obtained by considering $u_n - u_{n-1} << d$ and $w_n - w_{n-1} << d$ in Eqs. (7,8). By imposing a plane wave solution with wavenumber κ and angular frequency ω in Eqs. (35,36), the dispersion relations are

$$\omega_{\text{axial}}^2 = \frac{2K}{M}[1 - \cos(\kappa d)], \tag{37}$$

$$\omega_{\text{trans}}^2 = \frac{2P_0}{Md}[1 - \cos(\kappa d)]. \tag{38}$$

The governing equations of the classical continuum are obtained from a Taylor expansion of $u_{n\pm1}$ and $w_{n\pm1}$

$$u_{n\pm1} = u \pm du' + \frac{1}{2}d^2u'' + O(d^3), \tag{39}$$

$$w_{n\pm1} = w \pm dw' + \frac{1}{2}d^2w'' + O(d^3) \tag{40}$$

in Eqs. (35,36), leading to

$$\ddot{u} - c_1^2 u'' = 0, \tag{41}$$
$$\ddot{w} - c_2^2 w'' = 0. \tag{42}$$

If a plane wave solution is imposed to Eqs. (41,42), the dispersion relations are

$$\omega_{\text{axial}}^2 = c_1^2 \kappa^2, \tag{43}$$
$$\omega_{\text{trans}}^2 = c_2^2 \kappa^2. \tag{44}$$

The linear axiomatic continuum model is obtained by keeping the linear terms of Eqs. (29,30). Then, the governing equations are

$$\ddot{u} - \chi^2 \ddot{u}'' - c_1^2 u'' = 0, \tag{45}$$
$$\ddot{w} - \chi^2 \ddot{w}'' - c_2^2 w'' = 0. \tag{46}$$

By imposing a plane wave solution, we reach to the following dispersion relations

$$\omega_{\text{axial}}^2 = \frac{c_1^2 \kappa^2}{1 + \chi^2 \kappa^2}, \tag{47}$$
$$\omega_{\text{trans}}^2 = \frac{c_2^2 \kappa^2}{1 + \chi^2 \kappa^2}. \tag{48}$$

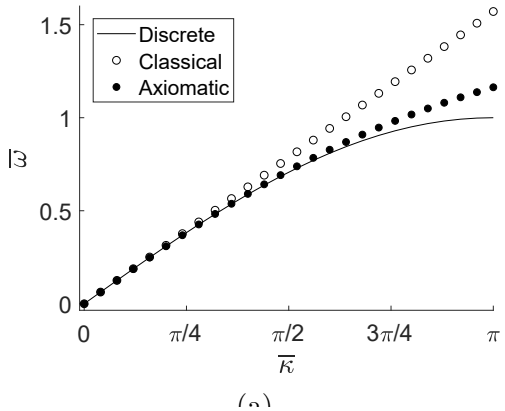

(b)

Figure 2: Linearized models: (a) Dispersion curves, (b) Difference in frequency between continuum and discrete models.

Fig. 2 shows the dispersion results obtained from the three linear models. Fig. 2a shows the dispersion curves for both axial and transverse displacements where frequency and wavenumber have been nondimensionalized as

$$\overline{\omega} = \omega/\omega_0 \qquad \overline{\kappa} = \kappa d \tag{49}$$

where ω_0 stands for the corresponding reference frequencies

$$\omega_{0,\text{axial}} = \sqrt{\frac{4K}{M}} = \frac{2c_1}{d}, \qquad \omega_{0,\text{trans}} = \sqrt{\frac{4P_0}{Md}} = \frac{2c_2}{d}. \tag{50}$$

Fig. 2b presents the relative difference in frequency between the continuum and discrete models calculated as

$$\overline{\mathcal{E}} = \frac{\overline{\omega}_{\text{Continuum}} - \overline{\omega}_{\text{Discrete}}}{\overline{\omega}_{\text{Discrete}}} \times 100. \tag{51}$$

As expected, the classical continuum is able to capture long-wavelength vibrations. As $\overline{\kappa}$ increases, the difference in frequency with the discrete model starts to be significant. For example, for a dimensionless wavenumber $\overline{\kappa} = \pi/2$, $\overline{\mathcal{E}} \approx 11\%$. Moreover, the axiomatic continuum model faithfully captures the discrete curve up to $\overline{\kappa} = \pi/2$ ($\overline{\mathcal{E}} \approx 1\%$). From this point on, the axiomatic model gives a considerable better approximation of the discrete model as compared to the classical one. Despite the good results given by the axiomatic continuum model, it is important to emphasize that these results are characteristics of the linear problems and, although there can be similarities, they may not translate to nonlinear regime.

6. Numerical solution of nonlinear discrete and continuum models

This section presents the methodologies for the solution of the discrete and axiomatic continuum model equations. The discrete model is solved using the Velocity Verlet algorithm [32], while the axiomatic model employs Galerkin Method. The time-response of the Galerkin solution is obtained with two methods: the first one, based on Jacobi's elliptical functions, permits to obtain an analytical solution, while the second, based on perturbation methods, leads to a closed-form solution.

Let us introduce the following nondimensional variables in Eqs. (33,34)

$$\varepsilon = \frac{c_2^2}{c_1^2} \ll 1, \quad \overline{u} = \frac{u}{\varepsilon L}, \quad \overline{w} = \frac{w}{\varepsilon L}, \quad \xi = \frac{X}{L}, \quad \tau = \omega_0 t, \quad \omega_0 = \frac{c_2}{L}, \quad h = \frac{\chi}{L}.$$

and consider from this point on $(\dot{\bullet}) \equiv \frac{\partial}{\partial \tau}$ and $(\bullet)' \equiv \frac{\partial}{\partial \xi}$. Eq. (34) transforms into

$$\ddot{\overline{w}} - h^2 \ddot{\overline{w}}'' - \overline{w}'' - \varepsilon \frac{\overline{w}''}{2} \int_0^1 \overline{w}'^2 d\xi = 0, \tag{52}$$

with boundary conditions

$$\overline{w}(0,\tau) = \overline{w}(1,\tau) = 0, \tag{53}$$

and initial conditions

$$\overline{w}(\xi,0) = \overline{w}_0(\xi), \qquad \dot{\overline{w}}(\xi,0) = 0, \tag{54}$$

where $\overline{w}_0(\xi)$ corresponds to the nondimensional expression of the continualized initial transverse displacement of the discrete model (Eq. (1)).

The proposed solution is

$$\overline{w}(\xi,\tau) = \sum_j q_j(\tau)\phi_j(\xi), \tag{55}$$

where $q_j(\tau)$ are the unknown time-dependent functions to be determined and $\phi_j(\xi)$ are the comparison functions, here chosen as

$$\phi_j(\xi) = \sin(\Omega_j \xi), \tag{56}$$

with $\Omega_j = j\pi$ $(j = 1, 2, 3, ...)$. Application of Galerkin method in Eq. (52)

$$(1 + h^2\Omega_j^2)\ddot{q}_j + \Omega_j^2(1 + \varepsilon\frac{\Omega_j^2}{4}\sum_h q_h^2)q_j = 0, \tag{57}$$

with initial conditions

$$q_j(0) = 2\int_0^1 \overline{w}_0(\xi)\phi_j(\xi)d\xi \tag{58}$$

and $\dot{q}_j(0) = 0$.

In case that the initial displacement condition $\overline{w}_0(\xi)$ is monochromatic and its wavenumber corresponds to a specific $\Omega_c = c\pi$,

$$\overline{w}_0(\xi) = q_0 \sin(c\pi\xi) \tag{59}$$

with amplitude q_0, the vector of initial conditions defined in Eq. (58) is zero except for $j = c$. Hence, the system (57) reduces to the single equation

$$\ddot{q} + \alpha q + \varepsilon\frac{\alpha\Omega^2}{4}q^3 = 0 \tag{60}$$

with

$$\alpha = \frac{\Omega^2}{1 + h^2\Omega^2} \tag{61}$$

and initial conditions $q(0) = q_0$ and $\dot{q}(0) = 0$, where subscripts c have been removed.

Eq. (60) corresponds to the undamped and unforced Duffing equation and an analytical solution via Jacobi's elliptical functions can be obtained [33]. Moreover, a perturbation method is used to solve Eq. (60) in order

to get a closed-form solution. The solution corresponding to the classical nonlinear model can be obtained for $h = 0$.

The analytical solution of the Duffing equation, Eq. (60) and initial conditions $q(0) = q_0$ and $\dot{q}(0) = 0$, makes use of Jacobi's elliptical function and is formulated as [33]

$$q(\tau) = q_0 \mathrm{cn}\left(\sqrt{\alpha + \beta q_0^2}\tau, \sqrt{\frac{\beta q_0^2}{2(\alpha + \beta q_0^2)}}\right) \tag{62}$$

with $\beta = \varepsilon\frac{\alpha\Omega^2}{4}$ and $\alpha + \beta q_0^2 \neq 0$. Function cn is Jacobi's elliptical cosine-function defined by [34]

$$\mathrm{cn}(\eta, m) = \cos\varphi, \tag{63}$$

where

$$\eta = \int_0^{\varphi} \frac{d\theta}{\sqrt{1 - m^2 \sin^2\theta}}. \tag{64}$$

The dimensionless frequency $\overline{\omega}$ of $q(\tau)$ is obtained by

$$\overline{\omega} = 2\pi/\mathcal{T}, \tag{65}$$

where the period $\mathcal{T}$ is

$$\mathcal{T} = \frac{4}{\sqrt{\alpha + \beta q_0^2}} \int_0^{\pi/4} \frac{d\theta}{\sqrt{1 - m^2 \sin^2\theta}}. \tag{66}$$

The influence of the dimensionless length-scale parameter h on the temporal evolution of function q, as well as on the dimensionless frequency $\overline{\omega}$, is presented in Fig. 3 for $\Omega = \pi$, $\varepsilon = 0.002$, and $q_0 = 0.05$. Fig. 3a shows that as h increases, the semi-period of the time-response also increases, which decreases $\overline{\omega}$ (Fig. 3b). Note that the time-response solution for $h = 0$ in Fig. 3a corresponds to the classical continuum model.

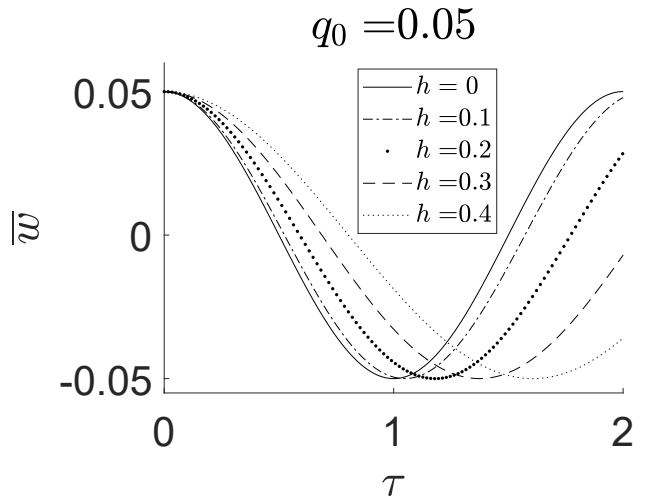

(a)

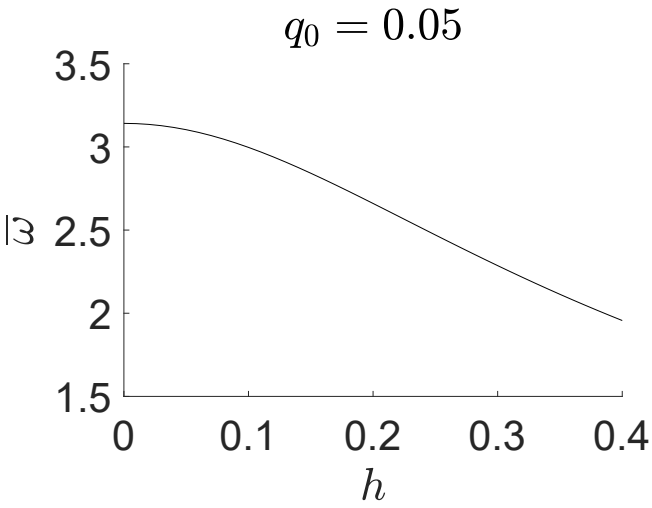

(b)

Figure 3: Analytical solution of the proposed axiomatic continuum model. Influence of the parameter h: (a) Time-dependent function q versus non-dimensional time τ, (b) Dimensionless frequency $\overline{\omega}$ vs parameter h.

A closed-form solution of the Duffing Eq. (60) and initial conditions $q(0) = q_0$ and $\dot{q}(0) = 0$ is now obtained employing the Multiple Scales method [35]. We seek a solution in the form

$$q = q^0 + \varepsilon q^1 + O(\varepsilon^2). \tag{67}$$

The time variable is expanded as $\tau^0 = \tau$ and $\tau^1 = \varepsilon\tau$. Introducing these expansions in Eq. (60), keeping terms up to $O(\varepsilon)$, and neglecting secular terms gives

$$q(\tau) = \hat{a}\cos(\overline{\omega}\tau + \hat{b}_0) + \varepsilon\frac{\hat{a}^3\Omega^2}{128}\cos(3\overline{\omega}\tau + 3\hat{b}_0), \tag{68}$$

with dimensionless frequency $\overline{\omega}$ and constant parameters $\hat{a}$ and $\hat{b}_0$. For the considered initial conditions, $\hat{a} = q_0$ and $\hat{b}_0 = 0$, hence,

$$q(\tau) = q_0\cos(\overline{\omega}\tau) + \varepsilon\frac{q_0^3\Omega^2}{128}\cos(3\overline{\omega}\tau), \tag{69}$$

with

$$\overline{\omega} = \sqrt{\alpha}\Big(1 + \varepsilon\frac{3\Omega^2}{32}q_0^2\Big). \tag{70}$$

The nondimensional form of Eq. (33) is

$$\overline{u}(\xi,\tau) = \frac{\varepsilon}{2}\xi\int_0^1 \overline{w}'^2 d\xi - \frac{\varepsilon}{2}\int_0^\xi \overline{w}'^2 d\xi \tag{71}$$

which corresponds to the governing equation of the dimensionless axial displacement which is driven by the transverse one. For

$$\overline{w}(\xi,\tau) = q(\tau)\sin(\Omega\xi), \tag{72}$$

the dimensionless axial displacement (Saad et al. [36], Leissa et al. [30]) reduces to

$$\overline{u}(\xi,\tau) = -\frac{\Omega}{8}\varepsilon q(\tau)^2\Big(\sin(2\Omega\xi) - \xi\sin(2\Omega)\Big). \tag{73}$$

In Eq. (73), $q(\tau)$ corresponds to the expression obtained with the Jacobi's elliptical functions (Eq. (62)) or through the perturbation method (Eq.(69)). Thus, for the discrete system, the initial condition in u_n should be consistent with the following expressions

$$\overline{u}_0(\xi) = \overline{u}(\xi,0) = -\frac{\Omega}{8}\varepsilon q_0^2\Big(\sin(2\Omega\xi) - \xi\sin(2\Omega)\Big), \qquad \dot{\overline{u}}(\xi,0) = 0. \tag{74}$$

7. Analysis of results

In this section we will compare the results obtained from three different approaches: classical and axiomatic continuum, and discrete model considered as the reference. We analyze the nonlinear vibration of a long chain of identical particles of mass M separated by a distance d and connected by linear springs with stiffness K. We consider as initial condition a sinusoidal transverse displacement with wavelength λ, which is varied to study its influence on the chain response. The initial axial displacement in Eq. (74) is considered.

Instead of the whole chain, we will solve a fully equivalent problem with a reduced number of particles. Then if a multiple of the semi-wavelength equals the distance between two given particles in the reference position $\left(m\frac{\lambda}{2} = (N+1)d\right)$ the considered problem is equivalent to a chain of length $L = (N+1)d$, corresponding to $N+2$ particles with fixed ends (defined in Section 2).

With the aim of reaching values of wavenumber $\overline{\kappa}$ close to π, we will consider an equivalent chain with $L = 3\frac{\lambda}{2}$, thus $m = 3$. Therefore, modifying the number of particles in the considered model, the wavelength λ and the dimensionless length-scale parameter h can be varied. A large number of particles would be representative of a problem with weak influence of the length scale, while a small number permits to study sharp size effects. Additionally, the amplitude of the initial displacement is increased to show the influence of the nonlinearity in the response.

Summarizing, the study is performed for the following values: $N = [23, 11, 5, 3]$ (see Fig. 4), $q_0 = [0.05, 0.5, 1, 1.5, 2, 2.5]$, and $\varepsilon = 0.002$. The considered initial transverse conditions for the discrete model are

$$w_n(0) = W_0(X_n) = \varepsilon L q_0 \sin\left(\frac{3\pi}{L}X_n\right), \quad \dot{w}_n(0) = 0, \tag{75}$$

which is paired with the following initial axial conditions

$$u_n(0) = U_0(X_n) = -\frac{3\pi}{8}\varepsilon^2 L q_0^2 \sin\left(\frac{6\pi}{L}X_n\right), \quad \dot{u}_n(0) = 0. \tag{76}$$

Consistently, the initial conditions for the continuum models are

$$\overline{w}_0(\xi) = \overline{w}(\xi, 0) = q_0 \sin(3\pi\xi), \qquad \dot{\overline{w}}(\xi, 0) = 0, \tag{77}$$

$$\overline{u}_0(\xi) = \overline{u}(\xi, 0) = -\frac{3\pi}{8}\varepsilon q_0^2 \sin(6\pi\xi), \qquad \dot{\overline{u}}(\xi, 0) = 0. \tag{78}$$

thus $\Omega = 3\pi$. The time-responses of the discrete and continuum models are obtained following the methodology explained in Section 6. The analytical solution given by Eq. (62) is used for the response of the continuum models. The perturbation solution, which provides valuable closed-form expressions, shows equivalent results, thus it will not be presented in the Figures. The analysis focuses on the transverse displacements, nevertheless a brief discussion about the results of the axial displacement is also provided.

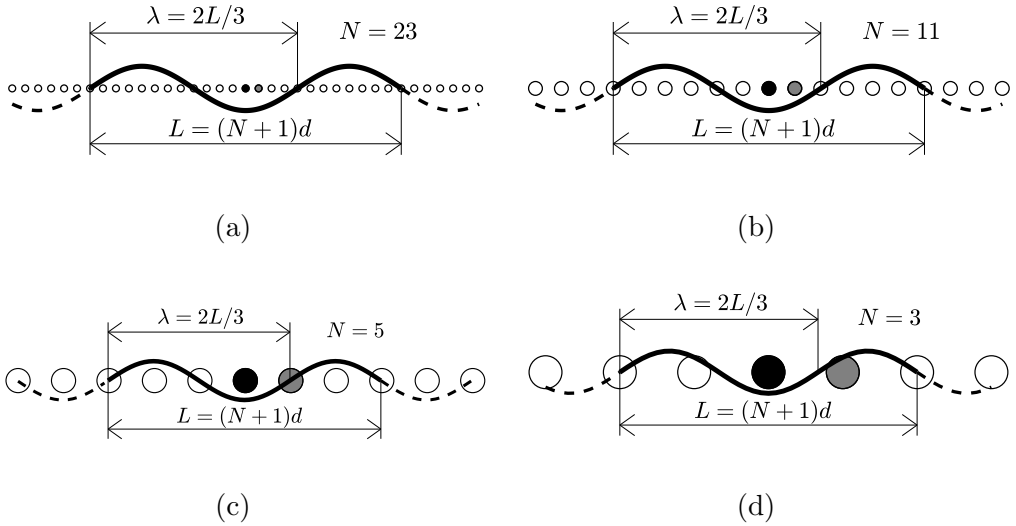

Figure 4: Discrete model. Sketch with equivalent problems and initial transverse displacements: (a) $N = 23$, (b) $N = 11$, (c) $N = 5$, and (d) $N = 3$. Central particle in black and neighboring particle on the right in gray.

7.1. Analysis of the transverse displacement

Figs. 5-8 compare, for different values of N, the time evolution of the dimensionless transverse displacement corresponding to the central particle ($n = \frac{N+3}{2}$, see Fig. 4) of the discrete model, which is the point at $\xi = 1/2$ in the continuum models.

Fig. 5 shows the results for $N = 23$ for different values of the amplitude of the initial displacement q_0. This study corresponds to wavenumber $\overline{\kappa} = \pi/8$ and scale parameter $h = 0.012$. As expected, the classical model is able to capture the response of the discrete one for this case of long-wavelength and small scale effect. For larger values of N, the scale effect becomes irrelevant and no differences are found among the different models.

Figs. 6-8 shows the dimensionless displacement for $N = [11, 5, 3]$ which correspond to $\overline{\kappa} = [\pi/4, \pi/2, 3\pi/4]$ and $h = [0.024, 0.048, 0.072]$, respectively. As N decreases, the wavelength becomes shorter and the scale effect starts to play a relevant role. For $N = 11$ (Fig. 6) differences between the classical model and the discrete start to be noticeable. However, the axiomatic model is able to capture the response of the discrete model. For $N = 5$ (Fig. 7) significant differences appear between the dimensionless displacement of the classical model and the discrete one. A good approximation is obtained with the axiomatic model, showing a better accuracy for any value of q_0. For $N = 3$, $\overline{\kappa} = 3\pi/4$ (Fig. 8) none of the continuum models is able to capture the response of the discrete model. However, the axiomatic one provides a much better approximation than the classical continuum model.

Fig. 9 shows the dimensionless frequency $\overline{\omega}$ of the corresponding transverse displacement versus q_0. The frequency of the discrete response is obtained from the Fast Fourier Transformation of transverse displacement of a particle. Eqs. (66,70) are used to obtain the frequencies of the continuum model from analytical, Eq. (66), and perturbation, Eq. (70), approaches. The figure shows that frequency increases with increasing values of q_0. For small values of q_0, the curve tends to be horizontal and the model reproduces the linear regime. As N decreases, the frequency of the responses of the discrete and axiomatic models decreases, meanwhile the frequency of classical model remains constant. This is the result of the absence of the length-scale parameter in the classical formulation. For $N = 23$ and $N = 11$, Figs. 9a-9b respectively, the axiomatic model faithfully captures the response of the discrete model while significant differences with the classical one start to appear. For a large number of particles, these differences are not present. As the wavelength becomes of the order of the microstructural dimension (Figs. 9c-9d), the axiomatic model gives a much better approximation to the discrete response than the classical model.

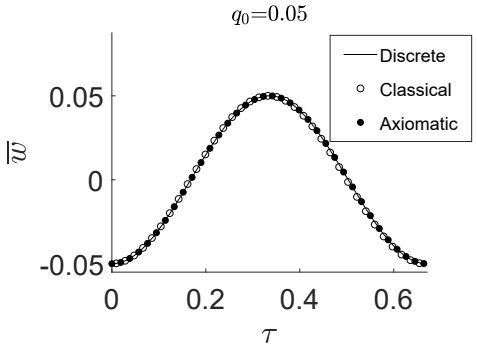

(a)

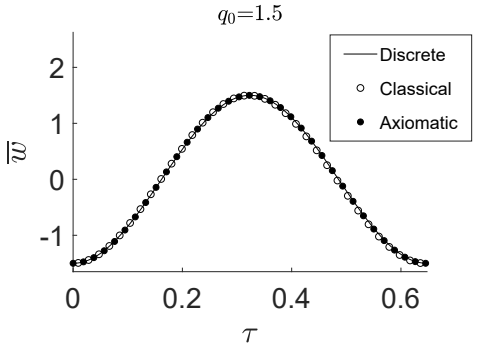

(b)

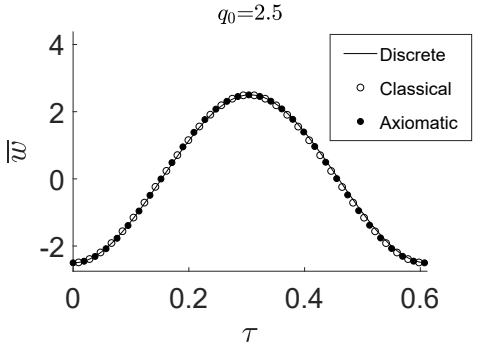

(c)

Figure 5: Discrete and continuum models. Dimensionless transverse displacement of central particle in the discrete model and $\overline{w}(1/2, \tau)$ in the continuum models for $N = 23$, $\overline{\kappa} = \pi/8$, $h = 0.012$ (axiom.), and: (a) $q_0 = 0.05$, (b) $q_0 = 1.5$, and (c) $q_0 = 2.5$.

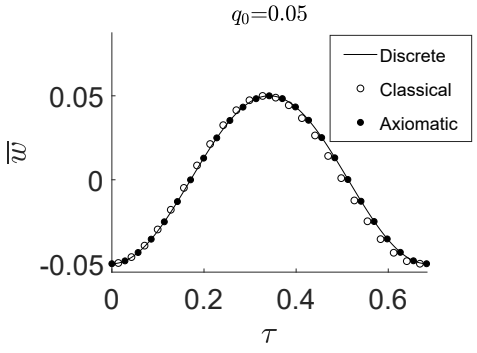

(a)

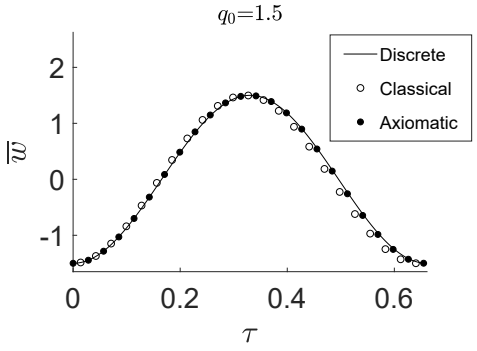

(b)

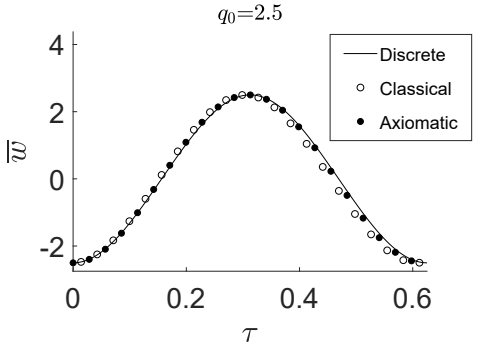

(c)

Figure 6: Discrete and continuum models. Dimensionless transverse displacement of central particle in the discrete model and $\overline{w}(1/2, \tau)$ in the continuum models for $N = 11$, $\overline{\kappa} = \pi/4$, $h = 0.024$ (axiom.), and: (a) $q_0 = 0.05$, (b) $q_0 = 1.5$, and (c) $q_0 = 2.5$.

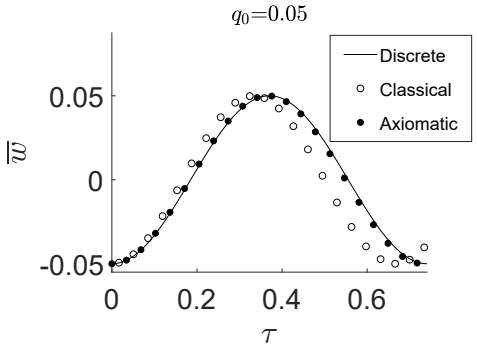

(a)

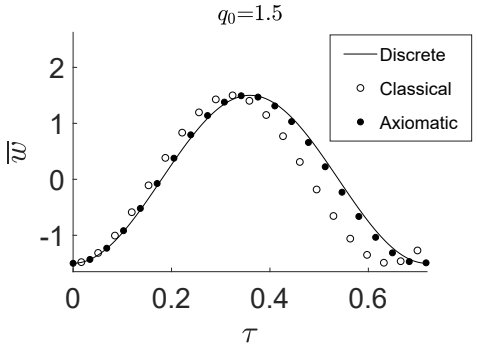

(b)

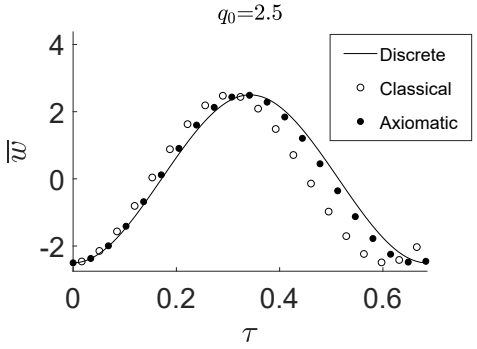

(c)

Figure 7: Discrete and continuum models. Dimensionless transverse displacement of central particle in the discrete model and $\overline{w}(1/2, \tau)$ in the continuum models for $N = 5$, $\overline{\kappa} = \pi/2$, $h = 0.048$ (axiom.), and: (a) $q_0 = 0.05$, (b) $q_0 = 1.5$, and (c) $q_0 = 2.5$.

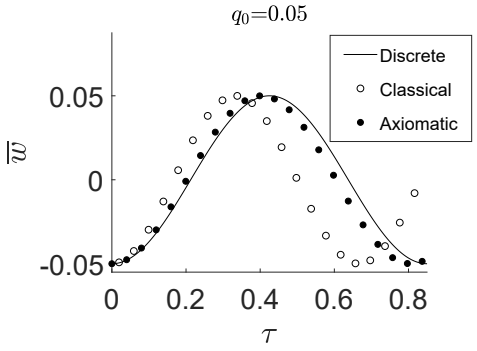

(a)

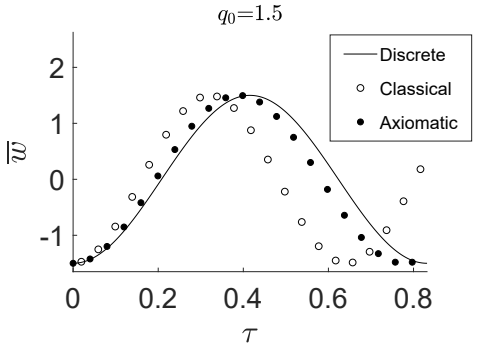

(b)

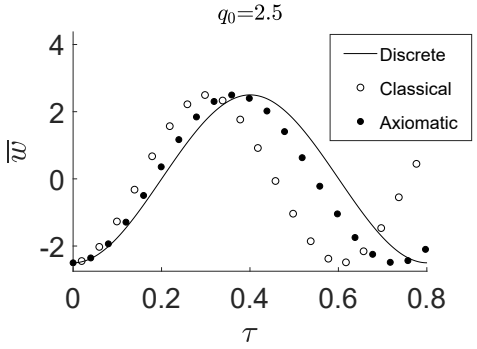

(c)

Figure 8: Discrete and continuum models. Dimensionless transverse displacement of central particle in the discrete model and $\overline{w}(1/2, \tau)$ in the continuum models for $N = 3$, $\overline{\kappa} = 3\pi/4$, $h = 0.072$ (axiom.), and: (a) $q_0 = 0.05$, (b) $q_0 = 1.5$, and (c) $q_0 = 2.5$.

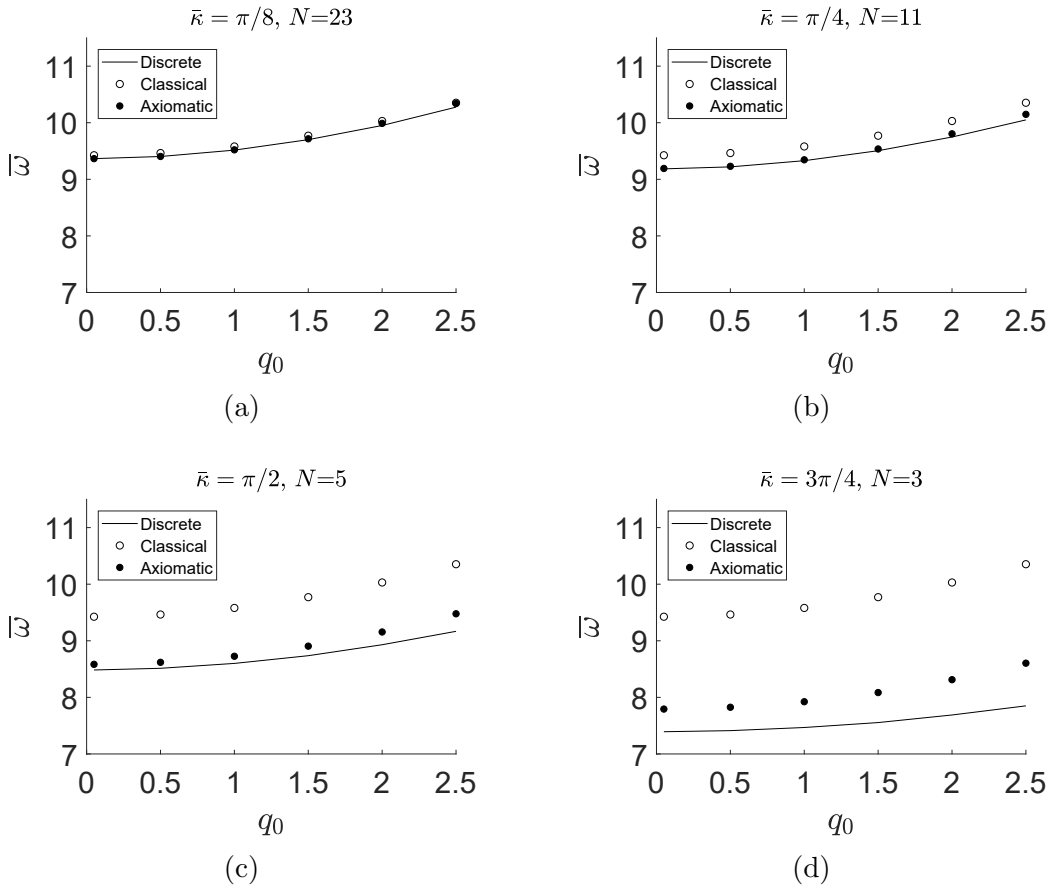

Figure 9: Discrete and continuum models. Dimensionless frequencies for: (a) $\overline{\kappa} = \pi/8$ and $N = 23$, (b) $\overline{\kappa} = \pi/4$ and $N = 11$, (c) $\overline{\kappa} = \pi/2$ and $N = 5$, and (d) $\overline{\kappa} = 3\pi/4$ and $N = 3$.

7.2. Analysis of the axial displacement

Fig. 10 compares, for $q_0 = 1$ and different values of $N = [23, 11, 3]$, the time evolution of the dimensionless axial displacement of the neighbor particle on the right of the central one ($n = \frac{N+3}{2}+1$, see Fig. 4) of the discrete model, which corresponds to the point $\xi = 1/2+1/(N+1)$ for the continuum models. The figure shows that for a large number of particles (Fig. 10a) the continuum models capture the response of the discrete model. For $N = 11$ (Fig. 10b), both classical and axiomatic models give a proper approximation of the discrete response, despite the presence of high-frequency harmonics in the discrete response. For $N = 3$ (Fig. 10c), the axial displacement of the discrete model is not captured by any of the continuum models. The reason is that the hypothesis of negligible axial acceleration is no longer valid, and thus Eq. (32) is not adequate to reproduce the axial behavior of the string.

It is important to highlight that the axial displacement is three orders of magnitude lower than the corresponding transverse one. Moreover, imposing an initial condition in the axial displacement different than the one given by Eq. (74) does not modify the transverse response as far as the amplitude of $\overline{u}$ is small, as it has been verified by additional calculations with the discrete model. Thus, the axiomatic model permits to capture the transverse displacement of the discrete regardless of the characteristics of the axial one.

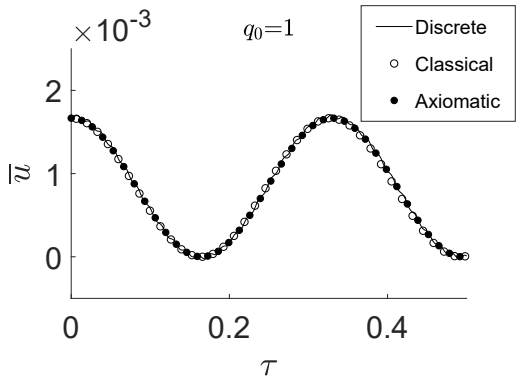

(a)

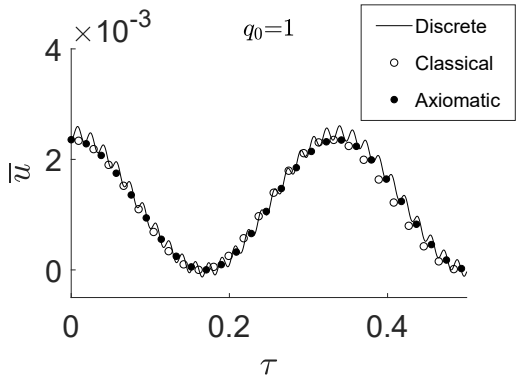

(b)

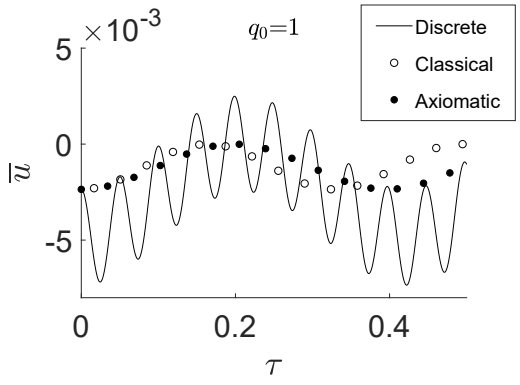

(c)

Figure 10: Discrete and continuum models. Dimensionless axial displacement of neighbor particle of the central one in the discrete model and $\overline{u}(1/2+1/(N+1),\tau)$ in the continuum models for $q_0 = 1$ and: (a) $\overline{\kappa} = \pi/8$ and $N = 23$, (b) $\overline{\kappa} = \pi/4$ and $N = 11$, and (c) $\overline{\kappa} = 3\pi/4$ and $N = 3$.

8. Conclusions

In this paper, an axiomatic continuum model has been developed to predict the response of a taut string with microstructure submitted to nonlinear axial and transverse vibrations. The model stems from an enrichment of the classical kinetic energy based on a inertia-gradient formulation and a classical potential energy. Starting from a non-standard continualization of the discrete problem, which accounts for scale effects, a relation between the parameters of the axiomatic and discrete models was established. A microstructure parameter was obtained, which permitted to take the scale effect into consideration. For a nil value of this parameter, the classical nonlinear continuum model was recovered. A comparison between the responses of the continuum models with that of the reference discrete one is provided to validate the proposed approach. This comparison shows the superiority of the axiomatic model over the classical one in capturing the scale effect. These have been the main findings:

- The axiomatic continuum model is able to reproduce the behavior of discrete model submitted to vibrations whose wavelength is of the order of the microstructural dimension. In these cases, the scale effect becomes relevant and the classical model is not suitable.

- The axiomatic continuum model always improves the results obtained using the classical one. The range of validity of this last model is approximately up to wavenumber $\overline{\kappa} = \pi/8$. The axiomatic continuum model obtains results equivalent to the discrete model up to $\overline{\kappa} = \pi/2$. Above this value, the axiomatic model gives a much better approximation than the classical continuum one.

- In the discrete and continuum models, higher initial amplitude leads to nonlinear behavior which leads to an increase in the frequency of the response with amplitude. However, an increase in the length-scale parameter plays the opposite role, leading to a marked decrease in frequency. While the proposed axiomatic model properly captures the influence of both amplitude and length scale, the classical model is not able to reproduce the second.

- The perturbation method provides closed-form equations for the time-response and frequency of the solution, obtaining a proper approxima-

tion to the analytical solution. Hence, it is an accurate straightforward solution for the time-response of the structured taut string.

Acknowledgments

M. Ruzzene acknowledges the support of the UC3M-Santander Chairs of Excellence Program during academic year 2017-18. This work was supported by the Ministerio de Economía y Competitividad de España (grant number DPI2014-57989-P).

References

[1] J. Li, C. Papadopoulos, J. Xu, Nanoelectronics: Growing Y-junction carbon nanotubes, Nature 402 (1999) 253.

[2] P. J. Burke, AC performance of nanoelectronics: towards a ballistic thz nanotube transistor, Solid-State Electronics 48 (2004) 1981–1986.

[3] T. J. Webster, M. C. Waid, J. L. McKenzie, R. L. Price, J. U. Ejiofor, Nano-biotechnology: carbon nanofibres as improved neural and orthopaedic implants, Nanotechnology 15 (2003) 48.

[4] V. S. Saji, H. C. Choe, K. W. Yeung, Nanotechnology in biomedical applications: a review, International Journal of Nano and Biomaterials 3 (2010) 119–139.

[5] V. Ghormade, M. V. Deshpande, K. M. Paknikar, Perspectives for nanobiotechnology enabled protection and nutrition of plants, Biotechnology advances 29 (2011) 792–803.

[6] E. Rousseau, A. Siria, G. Jourdan, S. Volz, F. Comin, J. Chevrier, J.-J. Greffet, Radiative heat transfer at the nanoscale, Nature Photonics 3 (2009) 5–14.

[7] T. Luo, G. Chen, Nanoscale heat transfer–from computation to experiment, Physical Chemistry Chemical Physics 15 (2013) 3389–3412.

[8] R. K. Pal, A. P. Awasthi, P. H. Geubelle, Wave propagation in elastoplastic granular systems, Granular Matter 15 (2013) 747–758.

[9] B. Jeong, H. Cho, H. Keum, S. Kim, D. M. McFarland, L. A. Bergman, W. P. King, A. F. Vakakis, Complex nonlinear dynamics in the limit of weak coupling of a system of microcantilevers connected by a geometrically nonlinear tunable nanomembrane, Nanotechnology 25 (2014) 465–501.

[10] A. M. Bouchaala, Size effect of a uniformly distributed added mass on a nanoelectromechanical resonator, Microsystem Technologies (2018) 1–10.

[11] J. Atalaya, J. M. Kinaret, A. Isacsson, Nanomechanical mass measurement using nonlinear response of a graphene membrane, EPL (Europhysics Letters) 91 (2010) 48001.

[12] S. S. Verbridge, J. M. Parpia, R. B. Reichenbach, L. M. Bellan, H. Craighead, High quality factor resonance at room temperature with nanostrings under high tensile stress, Journal of Applied Physics 99 (2006) 124304.

[13] V. Leiman, M. Ryzhii, A. Satou, N. Ryabova, V. Ryzhii, T. Otsuji, M. Shur, Analysis of resonant detection of terahertz radiation in high-electron mobility transistor with a nanostring/carbon nanotube as the mechanically floating gate, Journal of Applied Physics 104 (2008) 024–514.

[14] Y. Qin, X. Wang, Z. L. Wang, Microfibre–nanowire hybrid structure for energy scavenging, Nature 451 (2008) 809.

[15] A. Kudaibergenov, A. Nobili, L. Prikazchikova, On low-frequency vibrations of a composite string with contrast properties for energy scavenging fabric devices, Journal of Mechanics of Materials and Structures 11 (2016) 231–243.

[16] S. A. Nayfeh, A. H. Nayfeh, D. T. Mook, Nonlinear response of a taut string to longitudinal and transverse end excitation, Modal Analysis 1 (1995) 307–334.

[17] A. H. Nayfeh, D. T. Mook, Nonlinear oscillations, John Wiley & Sons, 2008.

[18] G. Anand, Large-amplitude damped free vibration of a stretched string, The Journal of the Acoustical Society of America 45 (1969) 1089–1096.

[19] H. Zhang, C. Wang, N. Challamel, Modelling vibrating nano-strings by lattice, finite difference and Eringen's nonlocal models, Journal of Sound and Vibration 425 (2018) 41–52.

[20] J. Vila, J. Fernández-Sáez, R. Zaera, Nonlinear continuum models for the dynamic behavior of 1D microstructured solids, International Journal of Solids and Structures 117 (2017) 111–122.

[21] J. Vila, J. Fernández-Sáez, R. Zaera, Reproducing the nonlinear dynamic behavior of a structured beam with a generalized continuum model, Journal of Sound and Vibration 420 (2018) 296–314.

[22] P. Rosenau, Dynamics of dense lattices, Physical Review B 36 (1987) 5868.

[23] P. Rosenau, Hamiltonian dynamics of dense chains and lattices: or how to correct the continuum, Physics Letters A 311 (2003) 39–52.

[24] R. D. Mindlin, Micro-structure in linear elasticity, Archive for Rational Mechanics and Analysis 16 (1964) 51–78.

[25] T. Doyle, J. L. Ericksen, Nonlinear elasticity, in: Advances in Applied Mechanics, Vol. 4, Elsevier, 1956, pp. 53–115.

[26] P. Germain, The method of virtual power in continuum mechanics. part 2: Microstructure, SIAM Journal on Applied Mathematics 25 (3) (1973) 556–575.

[27] H. Askes, E. C. Aifantis, Gradient elasticity theories in statics and dynamics-a unification of approaches, International journal of fracture 139 (2) (2006) 297–304.

[28] H. Askes, E. C. Aifantis, Gradient elasticity and flexural wave dispersion in carbon nanotubes, Physical Review B 80 (19) (2009) 195–412.

[29] S. Papargyri-Beskou, D. Polyzos, D. Beskos, Wave dispersion in gradient elastic solids and structures: a unified treatment, International Journal of Solids and Structures 46 (21) (2009) 3751–3759.

[30] A. Leissa, A. Saad, Large amplitude vibrations of strings, Journal of applied mechanics 61 (1994) 296–301.

[31] J. Gerstmayr, H. Irschik, On the correct representation of bending and axial deformation in the absolute nodal coordinate formulation with an elastic line approach, Journal of Sound and Vibration 318 (3) (2008) 461–487.

[32] N. S. Martys, R. D. Mountain, Velocity verlet algorithm for dissipative-particle-dynamics-based models of suspensions, Physical Review E 59 (3) (1999) 3733.

[33] A. Salas, J. Castillo, Exact solution to Duffing equation and the pendulum equation, Applied Mathematical Sciences 8 (2014) 8781–8789.

[34] M. Abramowitz, I. A. Stegun, Handbook of mathematical functions: with formulas, graphs, and mathematical tables, Vol. 55, Courier Corporation, 1964.

[35] A. H. Nayfeh, Introduction to perturbation techniques, John Wiley & Sons, 2011.

[36] A. M. Saad, Nonlinear free vibration analysis of strings by the galerkin method, Ph.D. thesis, The Ohio State University (1992).

Generalized continuum model for the analysis of nonlinear vibrations of taut strings with microstructure

Ó. Serrano[a,*], R. Zaera[a], J. Fernández-Sáez[a], M. Ruzzene[b,c]

[a]*Department of Continuum Mechanics and Structural Analysis, University Carlos III of Madrid, Av. de la Universidad 30, 28911 Leganés, Madrid, Spain*
[b]*School of Aerospace Engineering, Georgia Institute of Technology, Atlanta, Georgia 30332, USA*
[c]*School of Mechanical Engineering, Georgia Institute of Technology, Atlanta, Georgia 30332, USA*

Abstract

Classical continuum models are unable to capture the response of a microstructured solid when the scale effect is relevant. In vibration analysis, this limitation appears when the solid undergoes vibrations of wavelength that approaches the characteristic length of the microstructure. A discrete model may be formulated to account for this effect, but this comes at the expenses of high computational costs. For example, scale effects are relevant in strings employed in sensing applications which often rely on information gathered in the nonlinear dynamic regime. In this work, we study the dynamic behavior of a taut string modeled as a lattice of particles linked to first neighbors by linear springs. We develop an inertia-gradient generalized continuum model of the chain, which undergoes nonlinear vibrations. Unlike the corresponding classical continuum model, enrichment of the kinetic energy density with the characteristic length of the microstructure permits the model to capture short-wavelength vibrations. Comparison of the response predicted by the continuum models highlights that the generalized model provides better estimations of the dynamic response of the considered microstructured string in the nonlinear regime and at short wavelengths.

Keywords: Scale effect, Gradient continuum model, Taut string, Nonlinear Vibration, Microstructure

*Corresponding author. E-mail address: oscar.serrano@uc3m.es

1. Introduction

Classical continuum models of solids permit a faithful representation of their mechanical behavior. This statement is true when the characteristic dimensions of the underlying microstructure is significantly smaller than the scale of observation. This is the case of common problems in engineering such as in the civil or mechanical industries. In contrast, there are other engineering fields where the scale of observation is of the order of the microstructure. This is the case of nano-(micro-)electronics [1, 2], nano-biotechnology [3, 4, 5], nano-thermodynamics [6, 7], or in problems involving granular and particulate media [8].

In recent years, the interest in the nonlinear regime of these nano-/micro-scale structures has been spanned by sensing applications, where the nonlinear behavior of nano-structures has the potential to enhance the information that can be obtained from the sensor. For example, Jeong et al. [9] have shown that when geometric nonlinearity is considered, nano- or micro-mechanical resonators can overcome the narrow bandwidth limitation of linear dynamic systems. Bouchaala [10] used a nonlinear formulation of a nano-electromechanical resonator for mass sensing while Atalaya et al. [11] have shown how nano-size graphene membranes can be used in the nonlinear regime for the determination of the mass and position of an added particle. While the above studies consider beam-type and membrane-type components, studies on nano-strings include the work of Verbridge et al. [12] who presented how the resonant frequency of nano-strings allow to measuring mass with sensitivity approaching a zeptogram. Leiman et al. [13] developed a device based on a nano-string for the detection of terahertz electromagnetic radiation. Other studies related to the use of nano-strings have been developed by Qin et al. [14] and Kudaibergenov et al. [15]. In these examples, as the nano-string deflects transversely, its length, and therefore its tension, increases. Hence, nonlinear terms are required to account for stretching in the equations of motion (Nayfeh et al. [16, 17]). In these cases, classical continuum models might offer an acceptable approximation of the response of the string for long-wavelength vibrations [18]. However, once the wavelength becomes comparable to the characteristic dimensions of the underlying microstructure, classical continuum models are not appropriate to take scale effects into consideration. In nano-structures such as nano-strings, considered here as a structure where the scale effect appears due to discreteness, the formulation of appropriate models is needed. Zhang et al. [19] account

for size effects by considering the string as a 1D lattice. However, this formulation has a high computational cost. In this respect, generalized continuum models turns out to be attractive [19].

In this paper we start from a lattice model of a taut string and propose an inertia-gradient generalized continuum model with the aim of obtaining an accurate response for nonlinear vibrations at wavelengths comparable to the microstructural length. For the development of this continuum model, the methodology previously employed by Vila et al. to study the nonlinear vibrations of 1D structured solids, namely rods [20] and beams [21], is now applied to a different structural typology such as the taut string. The model will be called *axiomatic* and it will be derived from postulated forms of both kinetic and potential energies. In contrast to the classical continuum model, the enriched one takes scale effects into consideration and permits to recover the response of the classical one when the scale effects are neglected. A comparison of the equations of the generalized model with those derived through a non-standard continualization of the discrete equations of the lattice model permits to establish a relation between the corresponding parameters. Moreover, the axiomatic continuum model considers axial and transverse displacements leading to geometric nonlinearities. Also, analytical solutions are given for the response of the nonlinear string. A comparison between the responses of the different continuum models with the reference discrete one is presented to validate the proposed approach. Finally, results for short wavelengths are presented to illustrate the range of validity of the proposed model.

The paper is organized as follows. Section 1 provides a brief introduction and Section 2 formulates the discrete problem. Section 3 describes the formulation of a non-standard continualization to the discrete problem. Section 4 develops the axiomatic continuum model and Section 5 compares the dispersion curves of the linearized models. Section 6 describes the methodologies used for deriving the solution of the different models considered in this work, both discrete and continuum. Section 7 illustrates the comparison between the discrete, classical continuum and axiomatic continuum models. Finally, Section 8 summarizes the results of the work.

2. Formulation of the discrete problem

In this section we extend the lattice model of the linear taut string with microstructure developed by Zhang et al. [19] to the nonlinear behavior and

considering both axial and transverse vibration. The discrete system consists of a pinned-pinned chain of $N+2$ identical particles of mass M equally spaced at distance d, considered as the characteristic length of the underlying microstructure. Hence, the total length of the chain is $L=(N+1)d$. The reference position of n-th particle is $X_n=(n-1)d$ and $Z_n=0$, with $n=1,2,...,N+2$, in X and Z directions, respectively. Particles are linked to first neighbors by linear springs of stiffness K and are allowed to move in both axial and transverse directions (see Fig. 1). The taut chain has tension P_0 in the reference position.

Let us denote the axial and transverse displacements for n-th particle at time t as $u_n(t)$ and $w_n(t)$, respectively. Boundary conditions are defined by $u_1=u_{N+2}=w_1=w_{N+2}=0$. Also, the following initial conditions are imposed to the chain:

$$u_n(0)=U_0(X_n), \qquad \dot{u}_n(0)=0, \qquad w_n(0)=W_0(X_n), \qquad \dot{w}_n(0)=0, \quad (1)$$

U_0 and W_0 being functions of the discrete values X_n that satisfy fixed boundary conditions at the ends.

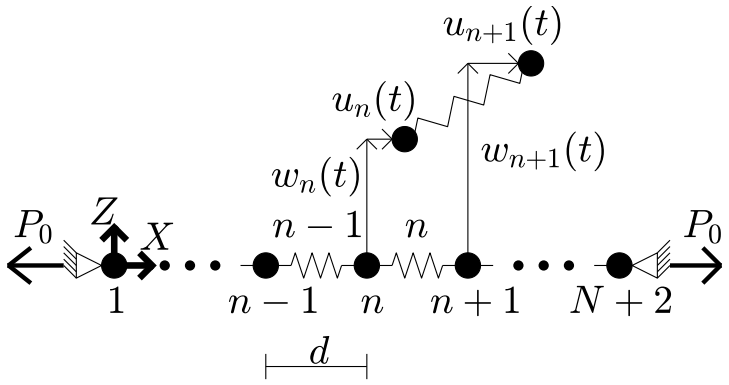

Figure 1: Sketch of the discrete model in reference and deformed position.

The kinetic energy $\mathbb{T}^{(n)}$ of the n-th particle and potential energy $\mathbb{W}^{(n)}$ of the n-th spring are defined by

$$\mathbb{T}^{(n)}_{\text{disc}}=\frac{1}{2}M\dot{u}_n^2+\frac{1}{2}M\dot{w}_n^2, \quad (2)$$

$$\mathbb{W}^{(n)}_{\text{disc}}=\frac{1}{2}K\Delta L_n^2+P_0\Delta L_n, \quad (3)$$

where $(\dot{\bullet})$ represents time-derivative, while ΔL_n is the elongation of the n-th spring (see Fig. 1), defined as

$$\Delta L_n = \sqrt{(u_{n+1} - u_n + d)^2 + (w_{n+1} - w_n)^2} - d. \tag{4}$$

The Lagrangian of the finite discrete model can be written as

$$\mathbb{L}_{\mathrm{D}} = \sum_n \mathbb{T}^{(n)}_{\mathrm{disc}} - \sum_n \mathbb{W}^{(n)}_{\mathrm{disc}}. \tag{5}$$

The stability of the equilibrium at the reference position can be demonstrated from the definition of the total potential energy (in absence of external loads)

$$\Pi_e = \sum_n \mathbb{W}^{(n)}_{\mathrm{disc}}, \tag{6}$$

since its first variation $\delta\Pi_e$ is zero and the second variation $\delta^2\Pi_e$ is strictly positive.

Moreover, applying Hamilton's Principle and the Fundamental Lemma of Variational Calculus leads to the following system of equations of motion for the particles

$$M\ddot{u}_n + (K\Delta L_{n-1} + P_0)\frac{d + u_n - u_{n-1}}{d + \Delta L_{n-1}} - (K\Delta L_n + P_0)\frac{d + u_{n+1} - u_n}{d + \Delta L_n} = 0, \tag{7}$$

$$M\ddot{w}_n + (K\Delta L_{n-1} + P_0)\frac{w_n - w_{n-1}}{d + \Delta L_{n-1}} - (K\Delta L_n + P_0)\frac{w_{n+1} - w_n}{d + \Delta L_n} = 0. \tag{8}$$

3. Non-standard continualization of the discrete problem

In this section we develop a non-standard continualization of the discrete system based on pseudo-differential operators [22, 23]. To this aim, we introduce the shift operator

$$\mathrm{e}^{d\partial_X} = 1 + d\partial_X + \frac{d^2}{2}\partial_X^2 + O(d^3) \tag{9}$$

which relates the displacements between neighboring particles as $u_{n+1} = \mathrm{e}^{d\partial_X} u_n$ and $w_{n+1} = \mathrm{e}^{d\partial_X} w_n$ ($\partial_X \equiv \frac{\partial}{\partial X}$). Let us define two variables $u(X,t)$, $w(X,t)$ as follows

$$\frac{\partial u}{\partial X} = \frac{u_{n+1} - u_n}{d}, \qquad \frac{\partial w}{\partial X} \equiv w' = \frac{w_{n+1} - w_n}{d}. \tag{10}$$

Variables $u(X,t)$ and $w(X,t)$ represent the continuum axial and transverse displacements at position X and time t, respectively. Then, a relation between the discrete and continuum variables can be established via Eqs. (9,10) as [23]

$$u_n = \mathbb{Q}u, \qquad w_n = \mathbb{Q}w \tag{11}$$

with

$$\mathbb{Q}(\partial_X) = \frac{d\partial_X}{\mathrm{e}^{d\partial_X} - 1} = 1 - \frac{d}{2}\partial_X + \frac{d^2}{12}\partial_X^2 + O(d^4).$$

The kinetic energy defined in Eq. (2) can now be expressed in terms of u and w by using the following relations proposed by Rosenau [23]

$$\dot{u}_n^2 = (\mathbb{Q}\dot{u}, \mathbb{Q}\dot{u}) = \int \dot{u}\mathbb{Q}^*\mathbb{Q}\dot{u}dX = \dot{u}^2 + \frac{d^2}{12}(\dot{u}')^2 + O(d^4), \tag{12}$$

$$\dot{w}_n^2 = (\mathbb{Q}\dot{w}, \mathbb{Q}\dot{w}) = \int \dot{w}\mathbb{Q}^*\mathbb{Q}\dot{w}dX = \dot{w}^2 + \frac{d^2}{12}(\dot{w}')^2 + O(d^4), \tag{13}$$

where $\mathbb{Q}^* = \mathbb{Q}(-\partial_X)$, while $(\bullet)'$ denotes derivative with respect to X. Then, by keeping terms up to order 2 in d, we obtain the approximate continuum Lagrangian

$$\mathbb{L}_{\mathrm{NS}} = \int_L \Big(\mathbb{T}_{\mathrm{cont}} - \mathbb{W}_{\mathrm{cont}}\Big)dX, \tag{14}$$

where

$$\mathbb{T}_{\mathrm{cont}} = \frac{1}{2}\frac{M}{d}\Big[\dot{u}^2 + \frac{d^2}{12}(\dot{u}')^2 + \dot{w}^2 + \frac{d^2}{12}(\dot{w}')^2\Big], \tag{15}$$

$$\mathbb{W}_{\mathrm{cont}} = \frac{1}{2}Kd(\sqrt{(u'+1)^2 + w'^2} - 1)^2 + P_0(\sqrt{(u'+1)^2 + w'^2} - 1). \tag{16}$$

Developing a Taylor-based asymptotic expansion to $\mathbb{W}_{\mathrm{cont}}$ up to fourth power terms of the derivatives, and applying Hamilton's Principle along with the Fundamental Lemma of Variational Calculus, leads to the continualized equations of motion of the discrete system

$$\ddot{u} - \frac{d^2}{12}\ddot{u}'' - \frac{Kd^2}{M}u'' - \Big(\frac{Kd^2}{M} - \frac{P_0 d}{M}\Big)\frac{\partial}{\partial X}\Big[w'^2\Big(\frac{1}{2} - u'\Big)\Big] = 0, \tag{17}$$

$$\ddot{w} - \frac{d^2}{12}\ddot{w}'' - \frac{P_0 d}{M}w'' - \Big(\frac{Kd^2}{M} - \frac{P_0 d}{M}\Big)\frac{\partial}{\partial X}\Big[w'(u' - u'^2 + \frac{1}{2}w'^2)\Big] = 0, \tag{18}$$

and the essential boundary conditions $u = 0$ and $w = 0$ at the ends.

In the next section, the governing equations of the axiomatic continuum model of a structured taut string will be compared with Eqs. (17,18) to establish a relation between the parameters of the discrete and axiomatic models.

4. Axiomatic continuum model

As stated before, classical continuum models are unable to capture the behavior of discrete problems when working with wavelengths of the order of the characteristic length of the underlying microstructure.

In this section a generalized continuum model of a taut string is presented. The model is formulated with a Mindlin-based kinetic energy [24] and a classical potential energy based on Biot strain and stress tensors [25]. The Mindlin micro-inertia term is expected to capture well wave dispersion phenomena in solids with microstructure, as stated by Mindlin [24] and Germain [26]. More recent literature related to this subject can be found in the works of Askes and Aifantis [27, 28] and Papargyri-Beskou et al. [29]. The potential energy is postulated by considering Biot strain which leads to strain expressions employed by other authors (Anand [18], Nayfeh et al. [16, 17] and Leissa et al. [30]) to obtain the governing equations of the classical nonlinear string. To this end, we first define $\mathbf{X}$ and $\mathbf{x}(\mathbf{X}, t)$ as the position vectors of a particle of the solid in the initial and current configurations, respectively. Then, the displacement vector $\mathbf{U}(\mathbf{X}, t)$ can be obtained as

$$\mathbf{U}(\mathbf{X}, t) = \mathbf{x}(\mathbf{X}, t) - \mathbf{X}. \tag{19}$$

The deformation gradient $\mathbf{F}$ can be written as follows

$$\mathbf{F} = \nabla[\mathbf{X} + \mathbf{U}(\mathbf{X}, t)] = \mathbf{I} + \nabla[\mathbf{U}(\mathbf{X}, t)], \tag{20}$$

where ∇ is the gradient operator with respect to $\mathbf{X}$, and $\mathbf{I}$ is the identity tensor.

The Biot strain tensor $\mathbf{e}$ [25] is defined as

$$\mathbf{e}(\mathbf{X}, t) = \sqrt{\mathbf{F}^{\mathrm{T}}\mathbf{F}} - \mathbf{I}. \tag{21}$$

The kinetic and potential energy densities are now postulated. The *kinetic energy density* is based on the Mindlin theory [24] which employs a scale

parameter χ, whose physical dimension is length, that accounts for the micro-inertia and the gradient of the velocities

$$\mathbb{T}_{\text{axiom}} = \frac{1}{2}\rho\Big[\frac{\partial \mathbf{U}}{\partial t}\cdot\frac{\partial \mathbf{U}}{\partial t} + \chi^2\frac{\partial(\nabla\mathbf{U})}{\partial t} : \frac{\partial(\nabla\mathbf{U})}{\partial t}\Big] \tag{22}$$

where ρ is the volumetric density. Also, "$\cdot$" and ":" denote the scalar product and the inner product, respectively. The typical values of χ are of the order of the characteristic dimension of the microstructure.

The *potential energy density* is based on the Biot strain tensor [25] and the potential energy introduced by the tension in the reference position through $\mathbf{T}_0$

$$\mathbb{W}_{\text{axiom}} = \frac{1}{2}\Lambda(\text{tr}\mathbf{e})^2 + \mu\mathbf{e} : \mathbf{e} + \mathbf{T}_0 : \mathbf{e} \tag{23}$$

with Lamé constants Λ and μ. Then, the Biot stress tensor including the stress component in the reference position is defined as

$$\mathbf{T}(\mathbf{X},t) = \frac{\partial \mathbb{W}}{\partial \mathbf{e}(\mathbf{X},t)} = \Lambda(\text{tr}\mathbf{e}(\mathbf{X},t))\mathbf{I} + 2\mu\mathbf{e}(\mathbf{X},t) + \mathbf{T}_0. \tag{24}$$

For the case of a unidimensional string undergoing axial and transverse displacements $\mathbf{U} = [u(X,t)\ w(X,t)]^T$, and the Biot strain is obtained by neglecting undesired deformation terms [31]

$$\text{e} = \sqrt{(1+u')^2 + w'^2} - 1. \tag{25}$$

If the string cross-section A is considered to remain undeformed (Poisson's ratio $\nu = 0$) and the stress in the reference position is $T_0 = P_0/A$, the kinetic $\mathbb{T}$ and potential $\mathbb{W}$ energy densities of the axiomatic continuum model are given by

$$\mathbb{T}_{\text{axiom}} = \frac{1}{2}\rho\Big[\dot{u}^2 + \dot{w}^2 + \chi^2(\dot{u}'^2 + \dot{w}'^2)\Big], \tag{26}$$

$$\mathbb{W}_{\text{axiom}} = \frac{1}{2}E\text{e}^2 + \frac{P_0}{A}\text{e} \tag{27}$$

with Young modulus E. As for the discrete model, it can be shown that the reference position is in stable equilibrium.

The Lagrangian of the axiomatic continuum model is obtained from

$$\mathbb{L}_{\text{AX}} = \int_L \mathbb{T}_{\text{axiom}} - \mathbb{W}_{\text{axiom}} dX. \tag{28}$$

Developing a Taylor-based asymptotic expansion to $\mathbb{W}_{\text{axiom}}$ up to fourth order and applying Hamilton's principle yields the governing equations for the axial and transverse displacements u and w

$$\ddot{u} - \chi^2 \ddot{u}'' - c_1^2 u'' - \left(c_1^2 - c_2^2\right) \frac{\partial}{\partial x} \left[w'^2 \left(\frac{1}{2} - u' \right) \right] = 0, \tag{29}$$

$$\ddot{w} - \chi^2 \ddot{w}'' - c_2^2 w'' - \left(c_1^2 - c_2^2\right) \frac{\partial}{\partial x} \left[w' (u' - u'^2 + \frac{1}{2} w'^2) \right] = 0, \tag{30}$$

where $c_1^2 = \frac{E}{\rho}$, $c_2^2 = \frac{P_0}{\rho A}$, with essential boundary conditions $u = 0$ and $w = 0$ at the ends. For $\chi = 0$, the classical nonlinear continuum equations of a nonlinear taut string are recovered (Nayfeh et al. [16]). It is important to highlight that the classical nonlinear continuum equations can be obtained from a Taylor-based continualization of Eqs. (7,8). This suggests that the considered lattice model is representative of the dynamic behavior of the string.

Let us compare continualized (17, 18) and axiomatic (29, 30) equations. It is straightforward to see that these equations are identical when

$$\frac{K d^2}{M} = \frac{E}{\rho}, \qquad \frac{M}{d} = \rho A, \qquad \frac{d^2}{12} = \chi^2. \tag{31}$$

Therefore, these relations establish the link between the discrete and continuum parameters. In particular, the scale parameter χ can be obtained from the physical characteristics of the discrete system. Anand et al. [18] and Nayfeh et al. [17] have shown the existence of interactions between axial and transverse modes of vibration. The i-th axial mode interacts with the j-th transverse one when $ic_1 \approx 2jc_2$. For the case of $c_2^2/c_1^2 << 1$ that is when the stiffness of the string EA is much higher than the tension P_0 in the reference position, and assuming lower-order transverse modes, this interaction is not present and the axial inertia $\ddot{u}$ (and $\ddot{u}''$) is therefore negligible (Nayfeh et al. [17]). Hence Eq. (29) can be approximated to

$$u'' = -\frac{\partial}{\partial X} \left[w'^2 \left(\frac{1}{2} - u' \right) \right]. \tag{32}$$

Integrating Eq. (32) twice by considering $w'^2 << 1$ and $u(0,t) = u(L,t) = 0$, gives

$$u = \frac{X}{2L} \int_0^L w'^2 dX - \frac{1}{2} \int_0^X w'^2 dX. \tag{33}$$

Finally, substituting Eq. (33) into Eq. (30), neglecting c_2^2 compared to c_1^2 and keeping cubic terms of w leads to the equation for transverse motion in the following form

$$\ddot{w} - \chi^2 \ddot{w}'' - c_2^2 w'' - \frac{c_1^2}{2L} w'' \int_0^L w'^2 dX = 0. \tag{34}$$

Note that Eq. (34) takes the scale effect under consideration. For $\chi = 0$, the corresponding nonlinear classical continuum equation after applying the above-mentioned assumptions is recovered [16, 17, 18].

5. Comparison of linear models

In this section we analyze the dispersion curves of the linear versions of the discrete, classical continuum and axiomatic continuum models. Even though the linear regime is here considered, the comparison between them provides an insight useful for the nonlinear regime.

The governing equations for the linear discrete model are

$$M\ddot{u}_n - K(u_{n+1} - 2u_n + u_{n-1}) = 0, \tag{35}$$

$$M\ddot{w}_n - \frac{P_0}{d}(w_{n+1} - 2w_n + w_{n-1}) = 0, \tag{36}$$

which are obtained by considering $u_n - u_{n-1} << d$ and $w_n - w_{n-1} << d$ in Eqs. (7,8). By imposing a plane wave solution with wavenumber κ and angular frequency ω in Eqs. (35,36), the dispersion relations are

$$\omega_{\text{axial}}^2 = \frac{2K}{M}[1 - \cos(\kappa d)], \tag{37}$$

$$\omega_{\text{trans}}^2 = \frac{2P_0}{Md}[1 - \cos(\kappa d)]. \tag{38}$$

The governing equations of the classical continuum are obtained from a Taylor expansion of $u_{n\pm1}$ and $w_{n\pm1}$

$$u_{n\pm1} = u \pm du' + \frac{1}{2}d^2u'' + O(d^3), \tag{39}$$

$$w_{n\pm1} = w \pm dw' + \frac{1}{2}d^2w'' + O(d^3) \tag{40}$$

in Eqs. (35,36), leading to

$$\ddot{u} - c_1^2 u'' = 0, \tag{41}$$
$$\ddot{w} - c_2^2 w'' = 0. \tag{42}$$

If a plane wave solution is imposed to Eqs. (41,42), the dispersion relations are

$$\omega_{\text{axial}}^2 = c_1^2 \kappa^2, \tag{43}$$
$$\omega_{\text{trans}}^2 = c_2^2 \kappa^2. \tag{44}$$

The linear axiomatic continuum model is obtained by keeping the linear terms of Eqs. (29,30). Then, the governing equations are

$$\ddot{u} - \chi^2 \ddot{u}'' - c_1^2 u'' = 0, \tag{45}$$
$$\ddot{w} - \chi^2 \ddot{w}'' - c_2^2 w'' = 0. \tag{46}$$

By imposing a plane wave solution, we reach to the following dispersion relations

$$\omega_{\text{axial}}^2 = \frac{c_1^2 \kappa^2}{1 + \chi^2 \kappa^2}, \tag{47}$$
$$\omega_{\text{trans}}^2 = \frac{c_2^2 \kappa^2}{1 + \chi^2 \kappa^2}. \tag{48}$$

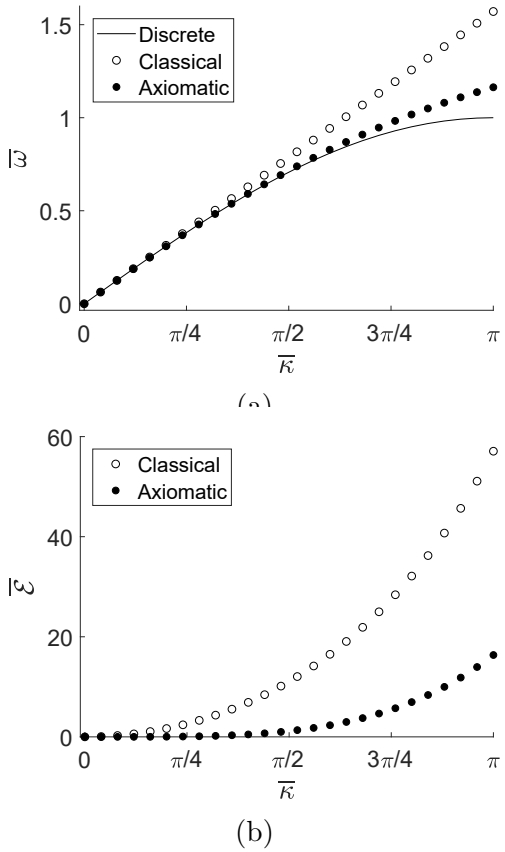

Figure 2: Linearized models: (a) Dispersion curves, (b) Difference in frequency between continuum and discrete models.

Fig. 2 shows the dispersion results obtained from the three linear models. Fig. 2a shows the dispersion curves for both axial and transverse displacements where frequency and wavenumber have been nondimensionalized as

$$\overline{\omega} = \omega/\omega_0 \qquad \overline{\kappa} = \kappa d \tag{49}$$

where ω_0 stands for the corresponding reference frequencies

$$\omega_{0,\text{axial}} = \sqrt{\frac{4K}{M}} = \frac{2c_1}{d}, \qquad \omega_{0,\text{trans}} = \sqrt{\frac{4P_0}{Md}} = \frac{2c_2}{d}. \tag{50}$$

Fig. 2b presents the relative difference in frequency between the continuum and discrete models calculated as

$$\overline{\mathcal{E}} = \frac{\overline{\omega}_{\text{Continuum}} - \overline{\omega}_{\text{Discrete}}}{\overline{\omega}_{\text{Discrete}}} \times 100. \tag{51}$$

As expected, the classical continuum is able to capture long-wavelength vibrations. As $\overline{\kappa}$ increases, the difference in frequency with the discrete model starts to be significant. For example, for a dimensionless wavenumber $\overline{\kappa} = \pi/2$, $\overline{\mathcal{E}} \approx 11\%$. Moreover, the axiomatic continuum model faithfully captures the discrete curve up to $\overline{\kappa} = \pi/2$ ($\overline{\mathcal{E}} \approx 1\%$). From this point on, the axiomatic model gives a considerable better approximation of the discrete model as compared to the classical one. Despite the good results given by the axiomatic continuum model, it is important to emphasize that these results are characteristics of the linear problems and, although there can be similarities, they may not translate to nonlinear regime.

6. Numerical solution of nonlinear discrete and continuum models

This section presents the methodologies for the solution of the discrete and axiomatic continuum model equations. The discrete model is solved using the Velocity Verlet algorithm [32], while the axiomatic model employs Galerkin Method. The time-response of the Galerkin solution is obtained with two methods: the first one, based on Jacobi's elliptical functions, permits to obtain an analytical solution, while the second, based on perturbation methods, leads to a closed-form solution.

Let us introduce the following nondimensional variables in Eqs. (33,34)

$$\varepsilon = \frac{c_2^2}{c_1^2} \ll 1, \quad \overline{u} = \frac{u}{\varepsilon L}, \quad \overline{w} = \frac{w}{\varepsilon L}, \quad \xi = \frac{X}{L}, \quad \tau = \omega_0 t, \quad \omega_0 = \frac{c_2}{L}, \quad h = \frac{\chi}{L}.$$

and consider from this point on $(\dot{\bullet}) \equiv \frac{\partial}{\partial \tau}$ and $(\bullet)' \equiv \frac{\partial}{\partial \xi}$. Eq. (34) transforms into

$$\ddot{\overline{w}} - h^2 \ddot{\overline{w}}'' - \overline{w}'' - \varepsilon \frac{\overline{w}''}{2} \int_0^1 \overline{w}'^2 d\xi = 0, \tag{52}$$

with boundary conditions

$$\overline{w}(0,\tau) = \overline{w}(1,\tau) = 0, \tag{53}$$

and initial conditions

$$\overline{w}(\xi,0) = \overline{w}_0(\xi), \qquad \dot{\overline{w}}(\xi,0) = 0, \tag{54}$$

where $\overline{w}_0(\xi)$ corresponds to the nondimensional expression of the continualized initial transverse displacement of the discrete model (Eq. (1)).

The proposed solution is

$$\overline{w}(\xi,\tau) = \sum_j q_j(\tau)\phi_j(\xi), \tag{55}$$

where $q_j(\tau)$ are the unknown time-dependent functions to be determined and $\phi_j(\xi)$ are the comparison functions, here chosen as

$$\phi_j(\xi) = \sin(\Omega_j \xi), \tag{56}$$

with $\Omega_j = j\pi$ $(j = 1, 2, 3, ...)$. Application of Galerkin method in Eq. (52)

$$(1 + h^2\Omega_j^2)\ddot{q}_j + \Omega_j^2(1 + \varepsilon\frac{\Omega_j^2}{4}\sum_h q_h^2)q_j = 0, \tag{57}$$

with initial conditions

$$q_j(0) = 2\int_0^1 \overline{w}_0(\xi)\phi_j(\xi)d\xi \tag{58}$$

and $\dot{q}_j(0) = 0$.

In case that the initial displacement condition $\overline{w}_0(\xi)$ is monochromatic and its wavenumber corresponds to a specific $\Omega_c = c\pi$,

$$\overline{w}_0(\xi) = q_0 \sin(c\pi\xi) \tag{59}$$

with amplitude q_0, the vector of initial conditions defined in Eq. (58) is zero except for $j = c$. Hence, the system (57) reduces to the single equation

$$\ddot{q} + \alpha q + \varepsilon\frac{\alpha\Omega^2}{4}q^3 = 0 \tag{60}$$

with

$$\alpha = \frac{\Omega^2}{1 + h^2\Omega^2} \tag{61}$$

and initial conditions $q(0) = q_0$ and $\dot{q}(0) = 0$, where subscripts c have been removed.

Eq. (60) corresponds to the undamped and unforced Duffing equation and an analytical solution via Jacobi's elliptical functions can be obtained [33]. Moreover, a perturbation method is used to solve Eq. (60) in order

to get a closed-form solution. The solution corresponding to the classical nonlinear model can be obtained for $h = 0$.

The analytical solution of the Duffing equation, Eq. (60) and initial conditions $q(0) = q_0$ and $\dot{q}(0) = 0$, makes use of Jacobi's elliptical function and is formulated as [33]

$$q(\tau) = q_0 \mathrm{cn}\left(\sqrt{\alpha + \beta q_0^2}\tau, \sqrt{\frac{\beta q_0^2}{2(\alpha + \beta q_0^2)}}\right) \tag{62}$$

with $\beta = \varepsilon\frac{\alpha\Omega^2}{4}$ and $\alpha + \beta q_0^2 \neq 0$. Function cn is Jacobi's elliptical cosine-function defined by [34]

$$\mathrm{cn}(\eta, m) = \cos\varphi, \tag{63}$$

where

$$\eta = \int_0^{\varphi} \frac{d\theta}{\sqrt{1 - m^2 \sin^2\theta}}. \tag{64}$$

The dimensionless frequency $\overline{\omega}$ of $q(\tau)$ is obtained by

$$\overline{\omega} = 2\pi/\mathcal{T}, \tag{65}$$

where the period $\mathcal{T}$ is

$$\mathcal{T} = \frac{4}{\sqrt{\alpha + \beta q_0^2}} \int_0^{\pi/4} \frac{d\theta}{\sqrt{1 - m^2 \sin^2\theta}}. \tag{66}$$

The influence of the dimensionless length-scale parameter h on the temporal evolution of function q, as well as on the dimensionless frequency $\overline{\omega}$, is presented in Fig. 3 for $\Omega = \pi$, $\varepsilon = 0.002$, and $q_0 = 0.05$. Fig. 3a shows that as h increases, the semi-period of the time-response also increases, which decreases $\overline{\omega}$ (Fig. 3b). Note that the time-response solution for $h = 0$ in Fig. 3a corresponds to the classical continuum model.

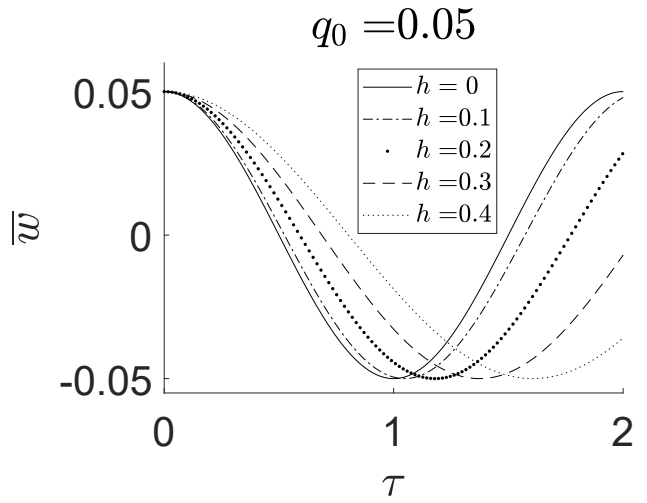

(a)

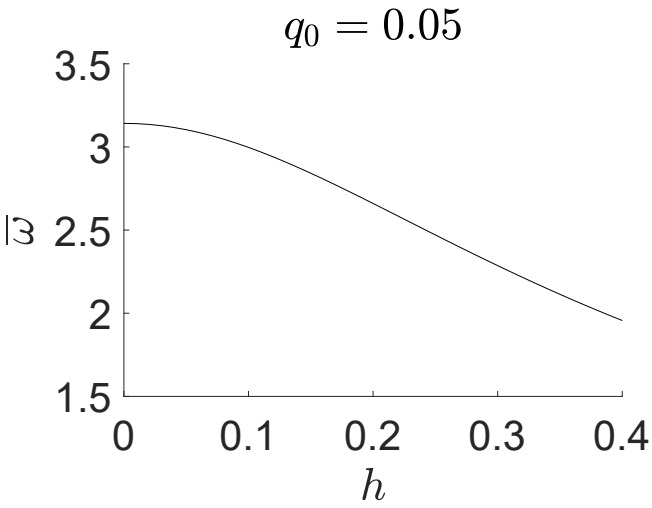

(b)

Figure 3: Analytical solution of the proposed axiomatic continuum model. Influence of the parameter h: (a) Time-dependent function q versus non-dimensional time τ, (b) Dimensionless frequency $\overline{\omega}$ vs parameter h.

A closed-form solution of the Duffing Eq. (60) and initial conditions $q(0) = q_0$ and $\dot{q}(0) = 0$ is now obtained employing the Multiple Scales method [35]. We seek a solution in the form

$$q = q^0 + \varepsilon q^1 + O(\varepsilon^2). \tag{67}$$

The time variable is expanded as $\tau^0 = \tau$ and $\tau^1 = \varepsilon\tau$. Introducing these expansions in Eq. (60), keeping terms up to $O(\varepsilon)$, and neglecting secular terms gives

$$q(\tau) = \hat{a}\cos(\overline{\omega}\tau + \hat{b}_0) + \varepsilon\frac{\hat{a}^3\Omega^2}{128}\cos(3\overline{\omega}\tau + 3\hat{b}_0), \tag{68}$$

with dimensionless frequency $\overline{\omega}$ and constant parameters $\hat{a}$ and $\hat{b}_0$. For the considered initial conditions, $\hat{a} = q_0$ and $\hat{b}_0 = 0$, hence,

$$q(\tau) = q_0\cos(\overline{\omega}\tau) + \varepsilon\frac{q_0^3\Omega^2}{128}\cos(3\overline{\omega}\tau), \tag{69}$$

with

$$\overline{\omega} = \sqrt{\alpha}\Big(1 + \varepsilon\frac{3\Omega^2}{32}q_0^2\Big). \tag{70}$$

The nondimensional form of Eq. (33) is

$$\overline{u}(\xi,\tau) = \frac{\varepsilon}{2}\xi\int_0^1 \overline{w}'^2 d\xi - \frac{\varepsilon}{2}\int_0^\xi \overline{w}'^2 d\xi \tag{71}$$

which corresponds to the governing equation of the dimensionless axial displacement which is driven by the transverse one. For

$$\overline{w}(\xi,\tau) = q(\tau)\sin(\Omega\xi), \tag{72}$$

the dimensionless axial displacement (Saad et al. [36], Leissa et al. [30]) reduces to

$$\overline{u}(\xi,\tau) = -\frac{\Omega}{8}\varepsilon q(\tau)^2\Big(\sin(2\Omega\xi) - \xi\sin(2\Omega)\Big). \tag{73}$$

In Eq. (73), $q(\tau)$ corresponds to the expression obtained with the Jacobi's elliptical functions (Eq. (62)) or through the perturbation method (Eq.(69)). Thus, for the discrete system, the initial condition in u_n should be consistent with the following expressions

$$\overline{u}_0(\xi) = \overline{u}(\xi,0) = -\frac{\Omega}{8}\varepsilon q_0^2\Big(\sin(2\Omega\xi) - \xi\sin(2\Omega)\Big), \qquad \dot{\overline{u}}(\xi,0) = 0. \tag{74}$$

7. Analysis of results

In this section we will compare the results obtained from three different approaches: classical and axiomatic continuum, and discrete model considered as the reference. We analyze the nonlinear vibration of a long chain of identical particles of mass M separated by a distance d and connected by linear springs with stiffness K. We consider as initial condition a sinusoidal transverse displacement with wavelength λ, which is varied to study its influence on the chain response. The initial axial displacement in Eq. (74) is considered.

Instead of the whole chain, we will solve a fully equivalent problem with a reduced number of particles. Then if a multiple of the semi-wavelength equals the distance between two given particles in the reference position $\left(m\frac{\lambda}{2} = (N+1)d\right)$ the considered problem is equivalent to a chain of length $L = (N+1)d$, corresponding to $N+2$ particles with fixed ends (defined in Section 2).

With the aim of reaching values of wavenumber $\overline{\kappa}$ close to π, we will consider an equivalent chain with $L = 3\frac{\lambda}{2}$, thus $m = 3$. Therefore, modifying the number of particles in the considered model, the wavelength λ and the dimensionless length-scale parameter h can be varied. A large number of particles would be representative of a problem with weak influence of the length scale, while a small number permits to study sharp size effects. Additionally, the amplitude of the initial displacement is increased to show the influence of the nonlinearity in the response.

Summarizing, the study is performed for the following values: $N = [23, 11, 5, 3]$ (see Fig. 4), $q_0 = [0.05, 0.5, 1, 1.5, 2, 2.5]$, and $\varepsilon = 0.002$. The considered initial transverse conditions for the discrete model are

$$w_n(0) = W_0(X_n) = \varepsilon L q_0 \sin\left(\frac{3\pi}{L} X_n\right), \quad \dot{w}_n(0) = 0, \tag{75}$$

which is paired with the following initial axial conditions

$$u_n(0) = U_0(X_n) = -\frac{3\pi}{8}\varepsilon^2 L q_0^2 \sin\left(\frac{6\pi}{L} X_n\right), \quad \dot{u}_n(0) = 0. \tag{76}$$

Consistently, the initial conditions for the continuum models are

$$\overline{w}_0(\xi) = \overline{w}(\xi, 0) = q_0 \sin(3\pi\xi), \qquad \dot{\overline{w}}(\xi, 0) = 0, \tag{77}$$

$$\overline{u}_0(\xi) = \overline{u}(\xi, 0) = -\frac{3\pi}{8}\varepsilon q_0^2 \sin(6\pi\xi), \qquad \dot{\overline{u}}(\xi, 0) = 0. \tag{78}$$

thus $\Omega = 3\pi$. The time-responses of the discrete and continuum models are obtained following the methodology explained in Section 6. The analytical solution given by Eq. (62) is used for the response of the continuum models. The perturbation solution, which provides valuable closed-form expressions, shows equivalent results, thus it will not be presented in the Figures. The analysis focuses on the transverse displacements, nevertheless a brief discussion about the results of the axial displacement is also provided.

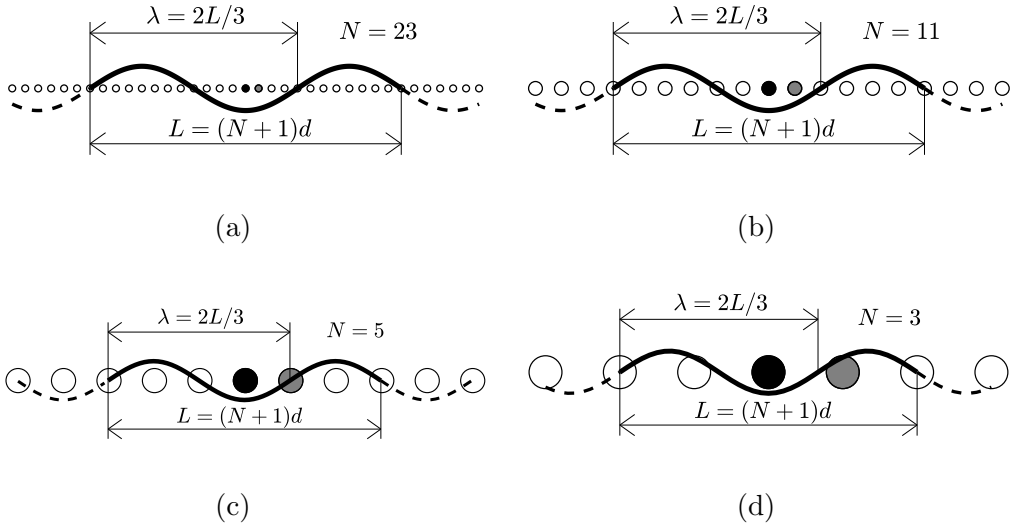

Figure 4: Discrete model. Sketch with equivalent problems and initial transverse displacements: (a) $N = 23$, (b) $N = 11$, (c) $N = 5$, and (d) $N = 3$. Central particle in black and neighboring particle on the right in gray.

7.1. Analysis of the transverse displacement

Figs. 5-8 compare, for different values of N, the time evolution of the dimensionless transverse displacement corresponding to the central particle ($n = \frac{N+3}{2}$, see Fig. 4) of the discrete model, which is the point at $\xi = 1/2$ in the continuum models.

Fig. 5 shows the results for $N = 23$ for different values of the amplitude of the initial displacement q_0. This study corresponds to wavenumber $\overline{\kappa} = \pi/8$ and scale parameter $h = 0.012$. As expected, the classical model is able to capture the response of the discrete one for this case of long-wavelength and small scale effect. For larger values of N, the scale effect becomes irrelevant and no differences are found among the different models.

Figs. 6-8 shows the dimensionless displacement for $N = [11, 5, 3]$ which correspond to $\overline{\kappa} = [\pi/4, \pi/2, 3\pi/4]$ and $h = [0.024, 0.048, 0.072]$, respectively. As N decreases, the wavelength becomes shorter and the scale effect starts to play a relevant role. For $N = 11$ (Fig. 6) differences between the classical model and the discrete start to be noticeable. However, the axiomatic model is able to capture the response of the discrete model. For $N = 5$ (Fig. 7) significant differences appear between the dimensionless displacement of the classical model and the discrete one. A good approximation is obtained with the axiomatic model, showing a better accuracy for any value of q_0. For $N = 3$, $\overline{\kappa} = 3\pi/4$ (Fig. 8) none of the continuum models is able to capture the response of the discrete model. However, the axiomatic one provides a much better approximation than the classical continuum model.

Fig. 9 shows the dimensionless frequency $\overline{\omega}$ of the corresponding transverse displacement versus q_0. The frequency of the discrete response is obtained from the Fast Fourier Transformation of transverse displacement of a particle. Eqs. (66,70) are used to obtain the frequencies of the continuum model from analytical, Eq. (66), and perturbation, Eq. (70), approaches. The figure shows that frequency increases with increasing values of q_0. For small values of q_0, the curve tends to be horizontal and the model reproduces the linear regime. As N decreases, the frequency of the responses of the discrete and axiomatic models decreases, meanwhile the frequency of classical model remains constant. This is the result of the absence of the length-scale parameter in the classical formulation. For $N = 23$ and $N = 11$, Figs. 9a-9b respectively, the axiomatic model faithfully captures the response of the discrete model while significant differences with the classical one start to appear. For a large number of particles, these differences are not present. As the wavelength becomes of the order of the microstructural dimension (Figs. 9c-9d), the axiomatic model gives a much better approximation to the discrete response than the classical model.

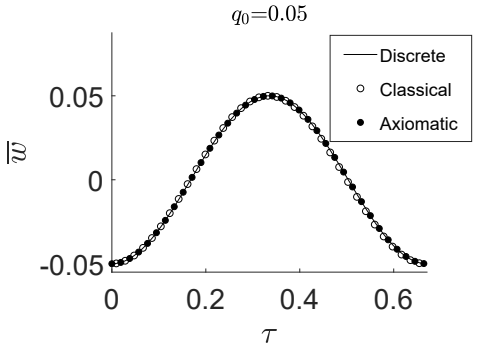

(a)

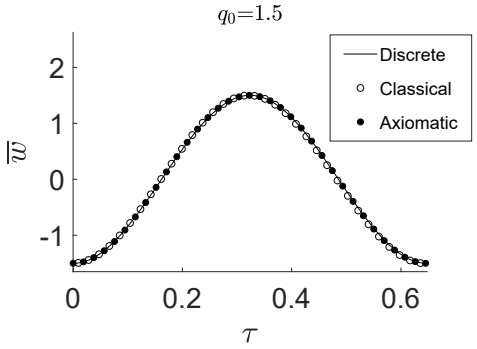

(b)

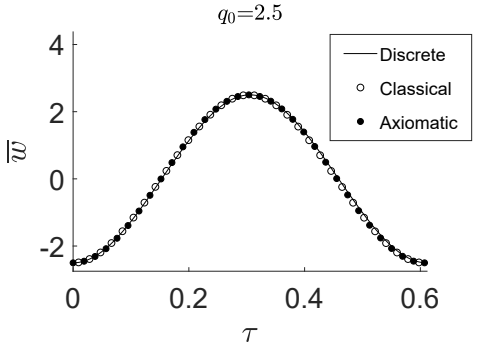

(c)

Figure 5: Discrete and continuum models. Dimensionless transverse displacement of central particle in the discrete model and $\overline{w}(1/2, \tau)$ in the continuum models for $N = 23$, $\overline{\kappa} = \pi/8$, $h = 0.012$ (axiom.), and: (a) $q_0 = 0.05$, (b) $q_0 = 1.5$, and (c) $q_0 = 2.5$.

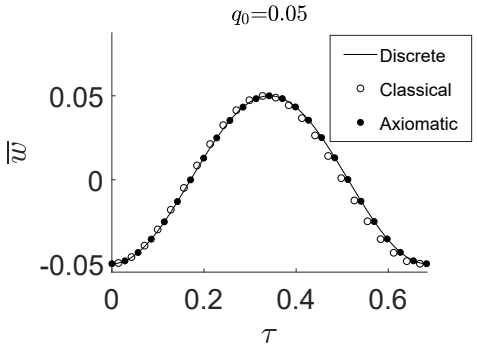

(a)

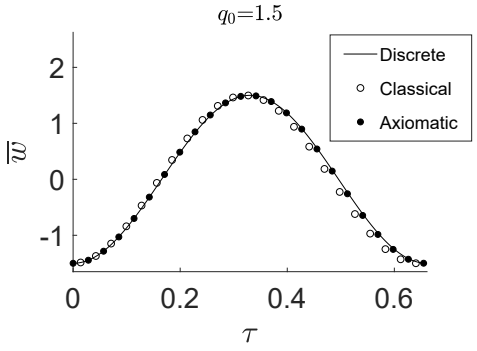

(b)

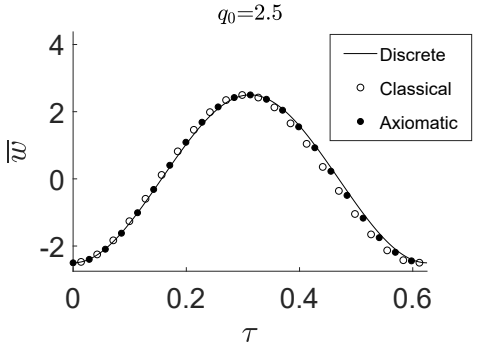

(c)

Figure 6: Discrete and continuum models. Dimensionless transverse displacement of central particle in the discrete model and $\overline{w}(1/2, \tau)$ in the continuum models for $N = 11$, $\overline{\kappa} = \pi/4$, $h = 0.024$ (axiom.), and: (a) $q_0 = 0.05$, (b) $q_0 = 1.5$, and (c) $q_0 = 2.5$.

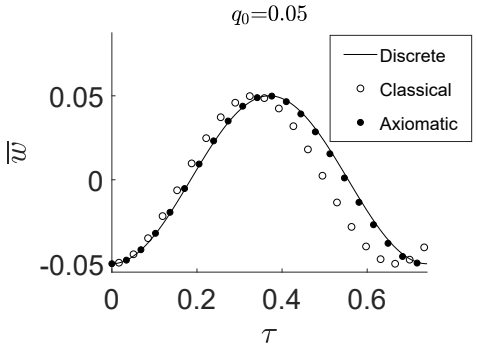

(a)

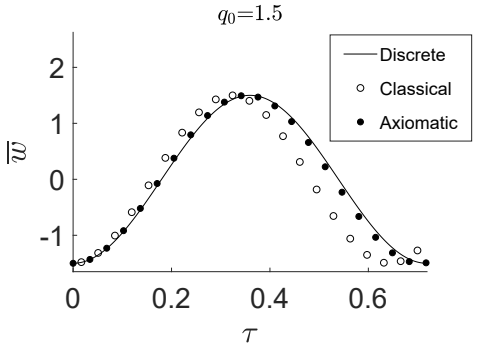

(b)

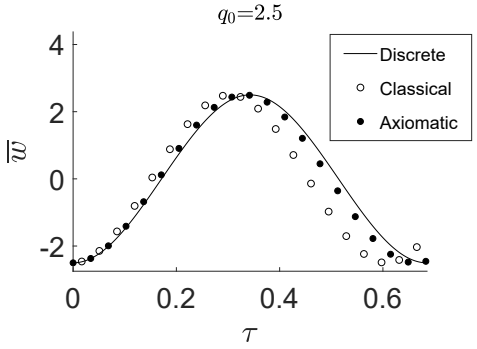

(c)

Figure 7: Discrete and continuum models. Dimensionless transverse displacement of central particle in the discrete model and $\overline{w}(1/2, \tau)$ in the continuum models for $N = 5$, $\overline{\kappa} = \pi/2$, $h = 0.048$ (axiom.), and: (a) $q_0 = 0.05$, (b) $q_0 = 1.5$, and (c) $q_0 = 2.5$.

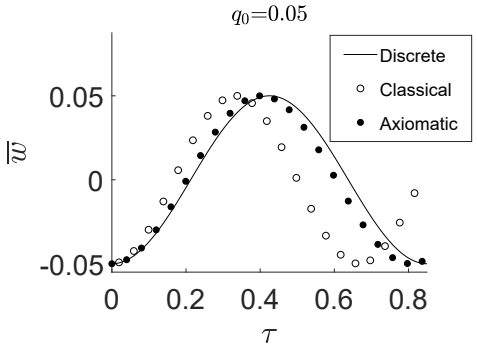

(a)

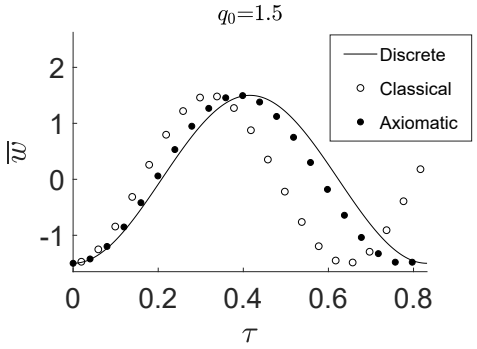

(b)

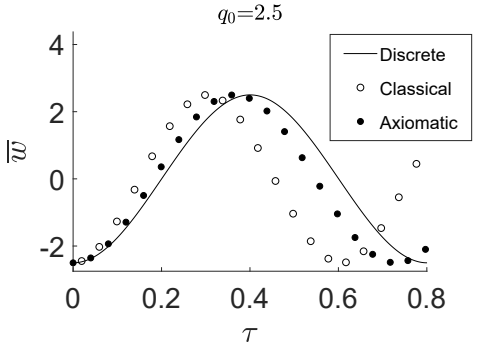

(c)

Figure 8: Discrete and continuum models. Dimensionless transverse displacement of central particle in the discrete model and $\overline{w}(1/2, \tau)$ in the continuum models for $N = 3$, $\overline{\kappa} = 3\pi/4$, $h = 0.072$ (axiom.), and: (a) $q_0 = 0.05$, (b) $q_0 = 1.5$, and (c) $q_0 = 2.5$.

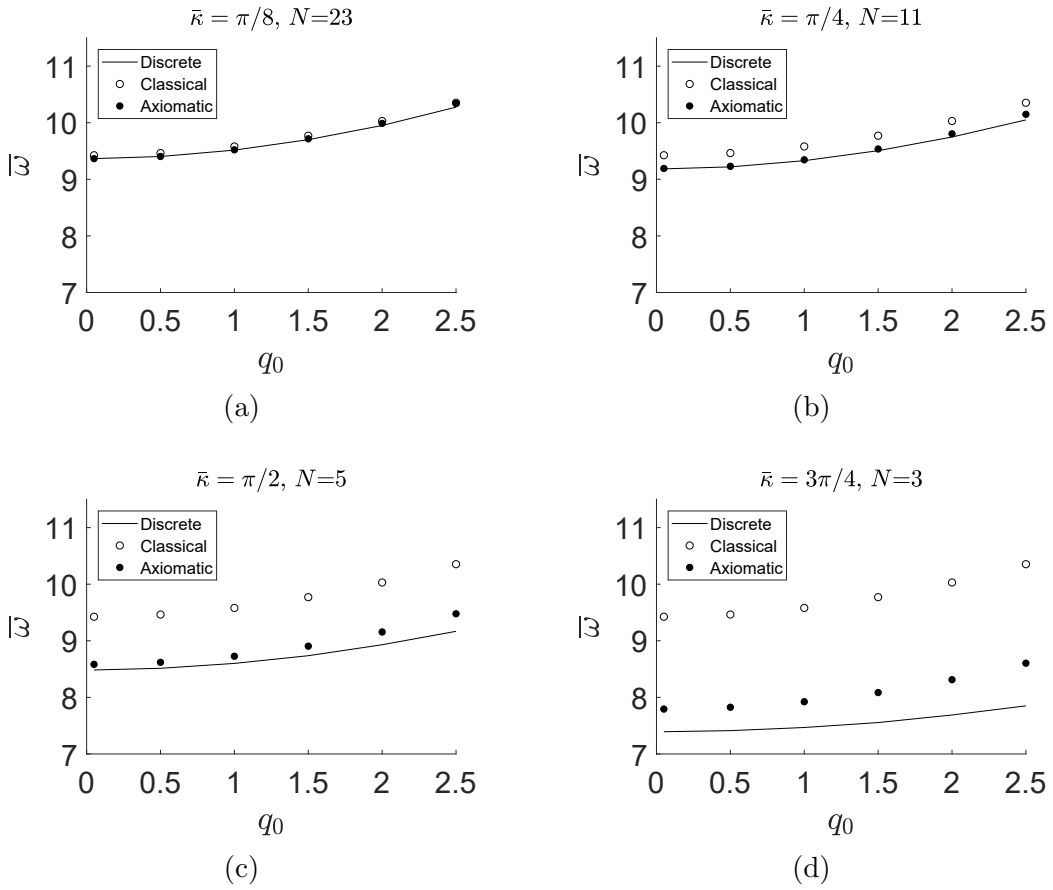

Figure 9: Discrete and continuum models. Dimensionless frequencies for: (a) $\overline{\kappa} = \pi/8$ and $N = 23$, (b) $\overline{\kappa} = \pi/4$ and $N = 11$, (c) $\overline{\kappa} = \pi/2$ and $N = 5$, and (d) $\overline{\kappa} = 3\pi/4$ and $N = 3$.

7.2. Analysis of the axial displacement

Fig. 10 compares, for $q_0 = 1$ and different values of $N = [23, 11, 3]$, the time evolution of the dimensionless axial displacement of the neighbor particle on the right of the central one ($n = \frac{N+3}{2}+1$, see Fig. 4) of the discrete model, which corresponds to the point $\xi = 1/2+1/(N+1)$ for the continuum models. The figure shows that for a large number of particles (Fig. 10a) the continuum models capture the response of the discrete model. For $N = 11$ (Fig. 10b), both classical and axiomatic models give a proper approximation of the discrete response, despite the presence of high-frequency harmonics in the discrete response. For $N = 3$ (Fig. 10c), the axial displacement of the discrete model is not captured by any of the continuum models. The reason is that the hypothesis of negligible axial acceleration is no longer valid, and thus Eq. (32) is not adequate to reproduce the axial behavior of the string.

It is important to highlight that the axial displacement is three orders of magnitude lower than the corresponding transverse one. Moreover, imposing an initial condition in the axial displacement different than the one given by Eq. (74) does not modify the transverse response as far as the amplitude of $\overline{u}$ is small, as it has been verified by additional calculations with the discrete model. Thus, the axiomatic model permits to capture the transverse displacement of the discrete regardless of the characteristics of the axial one.

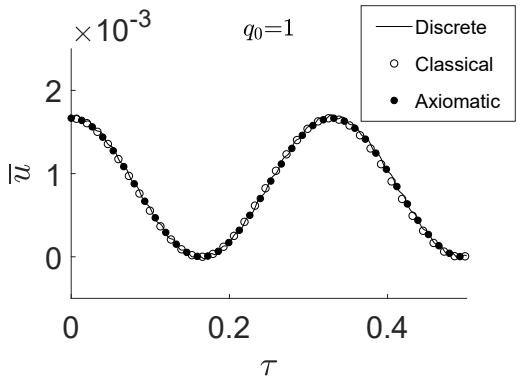

(a)

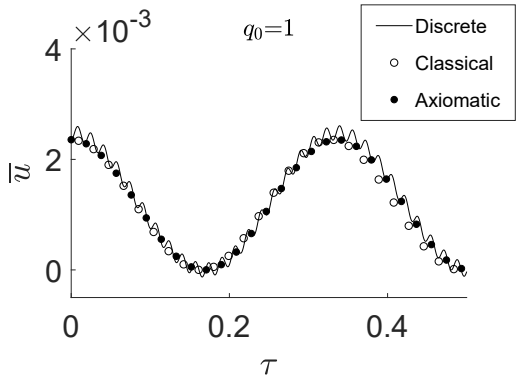

(b)

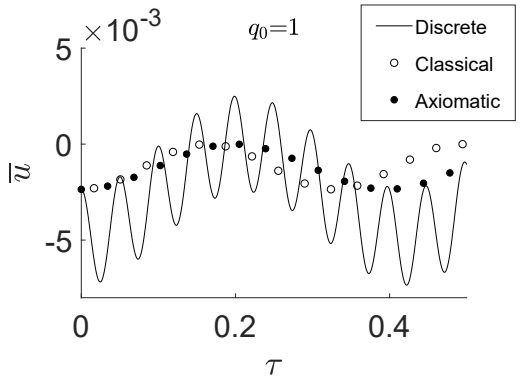

(c)

Figure 10: Discrete and continuum models. Dimensionless axial displacement of neighbor particle of the central one in the discrete model and $\overline{u}(1/2+1/(N+1),\tau)$ in the continuum models for $q_0 = 1$ and: (a) $\overline{\kappa} = \pi/8$ and $N = 23$, (b) $\overline{\kappa} = \pi/4$ and $N = 11$, and (c) $\overline{\kappa} = 3\pi/4$ and $N = 3$.

8. Conclusions

In this paper, an axiomatic continuum model has been developed to predict the response of a taut string with microstructure submitted to nonlinear axial and transverse vibrations. The model stems from an enrichment of the classical kinetic energy based on a inertia-gradient formulation and a classical potential energy. Starting from a non-standard continualization of the discrete problem, which accounts for scale effects, a relation between the parameters of the axiomatic and discrete models was established. A microstructure parameter was obtained, which permitted to take the scale effect into consideration. For a nil value of this parameter, the classical nonlinear continuum model was recovered. A comparison between the responses of the continuum models with that of the reference discrete one is provided to validate the proposed approach. This comparison shows the superiority of the axiomatic model over the classical one in capturing the scale effect. These have been the main findings:

- The axiomatic continuum model is able to reproduce the behavior of discrete model submitted to vibrations whose wavelength is of the order of the microstructural dimension. In these cases, the scale effect becomes relevant and the classical model is not suitable.

- The axiomatic continuum model always improves the results obtained using the classical one. The range of validity of this last model is approximately up to wavenumber $\overline{\kappa} = \pi/8$. The axiomatic continuum model obtains results equivalent to the discrete model up to $\overline{\kappa} = \pi/2$. Above this value, the axiomatic model gives a much better approximation than the classical continuum one.

- In the discrete and continuum models, higher initial amplitude leads to nonlinear behavior which leads to an increase in the frequency of the response with amplitude. However, an increase in the length-scale parameter plays the opposite role, leading to a marked decrease in frequency. While the proposed axiomatic model properly captures the influence of both amplitude and length scale, the classical model is not able to reproduce the second.

- The perturbation method provides closed-form equations for the time-response and frequency of the solution, obtaining a proper approxima-

tion to the analytical solution. Hence, it is an accurate straightforward solution for the time-response of the structured taut string.

Acknowledgments

M. Ruzzene acknowledges the support of the UC3M-Santander Chairs of Excellence Program during academic year 2017-18. This work was supported by the Ministerio de Economía y Competitividad de España (grant number DPI2014-57989-P).

References

[1] J. Li, C. Papadopoulos, J. Xu, Nanoelectronics: Growing Y-junction carbon nanotubes, Nature 402 (1999) 253.

[2] P. J. Burke, AC performance of nanoelectronics: towards a ballistic thz nanotube transistor, Solid-State Electronics 48 (2004) 1981–1986.

[3] T. J. Webster, M. C. Waid, J. L. McKenzie, R. L. Price, J. U. Ejiofor, Nano-biotechnology: carbon nanofibres as improved neural and orthopaedic implants, Nanotechnology 15 (2003) 48.

[4] V. S. Saji, H. C. Choe, K. W. Yeung, Nanotechnology in biomedical applications: a review, International Journal of Nano and Biomaterials 3 (2010) 119–139.

[5] V. Ghormade, M. V. Deshpande, K. M. Paknikar, Perspectives for nano-biotechnology enabled protection and nutrition of plants, Biotechnology advances 29 (2011) 792–803.

[6] E. Rousseau, A. Siria, G. Jourdan, S. Volz, F. Comin, J. Chevrier, J.-J. Greffet, Radiative heat transfer at the nanoscale, Nature Photonics 3 (2009) 5–14.

[7] T. Luo, G. Chen, Nanoscale heat transfer–from computation to experiment, Physical Chemistry Chemical Physics 15 (2013) 3389–3412.

[8] R. K. Pal, A. P. Awasthi, P. H. Geubelle, Wave propagation in elasto-plastic granular systems, Granular Matter 15 (2013) 747–758.

[9] B. Jeong, H. Cho, H. Keum, S. Kim, D. M. McFarland, L. A. Bergman, W. P. King, A. F. Vakakis, Complex nonlinear dynamics in the limit of weak coupling of a system of microcantilevers connected by a geometrically nonlinear tunable nanomembrane, Nanotechnology 25 (2014) 465–501.

[10] A. M. Bouchaala, Size effect of a uniformly distributed added mass on a nanoelectromechanical resonator, Microsystem Technologies (2018) 1–10.

[11] J. Atalaya, J. M. Kinaret, A. Isacsson, Nanomechanical mass measurement using nonlinear response of a graphene membrane, EPL (Europhysics Letters) 91 (2010) 48001.

[12] S. S. Verbridge, J. M. Parpia, R. B. Reichenbach, L. M. Bellan, H. Craighead, High quality factor resonance at room temperature with nanostrings under high tensile stress, Journal of Applied Physics 99 (2006) 124304.

[13] V. Leiman, M. Ryzhii, A. Satou, N. Ryabova, V. Ryzhii, T. Otsuji, M. Shur, Analysis of resonant detection of terahertz radiation in high-electron mobility transistor with a nanostring/carbon nanotube as the mechanically floating gate, Journal of Applied Physics 104 (2008) 024–514.

[14] Y. Qin, X. Wang, Z. L. Wang, Microfibre–nanowire hybrid structure for energy scavenging, Nature 451 (2008) 809.

[15] A. Kudaibergenov, A. Nobili, L. Prikazchikova, On low-frequency vibrations of a composite string with contrast properties for energy scavenging fabric devices, Journal of Mechanics of Materials and Structures 11 (2016) 231–243.

[16] S. A. Nayfeh, A. H. Nayfeh, D. T. Mook, Nonlinear response of a taut string to longitudinal and transverse end excitation, Modal Analysis 1 (1995) 307–334.

[17] A. H. Nayfeh, D. T. Mook, Nonlinear oscillations, John Wiley & Sons, 2008.

[18] G. Anand, Large-amplitude damped free vibration of a stretched string, The Journal of the Acoustical Society of America 45 (1969) 1089–1096.

[19] H. Zhang, C. Wang, N. Challamel, Modelling vibrating nano-strings by lattice, finite difference and Eringen's nonlocal models, Journal of Sound and Vibration 425 (2018) 41–52.

[20] J. Vila, J. Fernández-Sáez, R. Zaera, Nonlinear continuum models for the dynamic behavior of 1D microstructured solids, International Journal of Solids and Structures 117 (2017) 111–122.

[21] J. Vila, J. Fernández-Sáez, R. Zaera, Reproducing the nonlinear dynamic behavior of a structured beam with a generalized continuum model, Journal of Sound and Vibration 420 (2018) 296–314.

[22] P. Rosenau, Dynamics of dense lattices, Physical Review B 36 (1987) 5868.

[23] P. Rosenau, Hamiltonian dynamics of dense chains and lattices: or how to correct the continuum, Physics Letters A 311 (2003) 39–52.

[24] R. D. Mindlin, Micro-structure in linear elasticity, Archive for Rational Mechanics and Analysis 16 (1964) 51–78.

[25] T. Doyle, J. L. Ericksen, Nonlinear elasticity, in: Advances in Applied Mechanics, Vol. 4, Elsevier, 1956, pp. 53–115.

[26] P. Germain, The method of virtual power in continuum mechanics. part 2: Microstructure, SIAM Journal on Applied Mathematics 25 (3) (1973) 556–575.

[27] H. Askes, E. C. Aifantis, Gradient elasticity theories in statics and dynamics-a unification of approaches, International journal of fracture 139 (2) (2006) 297–304.

[28] H. Askes, E. C. Aifantis, Gradient elasticity and flexural wave dispersion in carbon nanotubes, Physical Review B 80 (19) (2009) 195–412.

[29] S. Papargyri-Beskou, D. Polyzos, D. Beskos, Wave dispersion in gradient elastic solids and structures: a unified treatment, International Journal of Solids and Structures 46 (21) (2009) 3751–3759.

[30] A. Leissa, A. Saad, Large amplitude vibrations of strings, Journal of applied mechanics 61 (1994) 296–301.

[31] J. Gerstmayr, H. Irschik, On the correct representation of bending and axial deformation in the absolute nodal coordinate formulation with an elastic line approach, Journal of Sound and Vibration 318 (3) (2008) 461–487.

[32] N. S. Martys, R. D. Mountain, Velocity verlet algorithm for dissipative-particle-dynamics-based models of suspensions, Physical Review E 59 (3) (1999) 3733.

[33] A. Salas, J. Castillo, Exact solution to Duffing equation and the pendulum equation, Applied Mathematical Sciences 8 (2014) 8781–8789.

[34] M. Abramowitz, I. A. Stegun, Handbook of mathematical functions: with formulas, graphs, and mathematical tables, Vol. 55, Courier Corporation, 1964.

[35] A. H. Nayfeh, Introduction to perturbation techniques, John Wiley & Sons, 2011.

[36] A. M. Saad, Nonlinear free vibration analysis of strings by the galerkin method, Ph.D. thesis, The Ohio State University (1992).